ELECTROMAGNETIC WAVE PROPAGATION IN A MAGNETIZED LABORATORY PLASMA

by

Michael Joseph Rowlands

Submitted to the Department of Electrical Engineering and Computer Science
in partial fulfillment of the requirements for the degrees of

Master of Engineering

and

Bachelor of Science

at the

MASSACHUSETTS INSTITUTE OF TECHNOLOGY

May 1998

Author .....
Department of Electrical Engineering and Computer Science
May 22, 1998

Certified by .....
Min-Chang Lee
Head of Ionospheric Plasma Research Group
Thesis Supervisor

Accepted by .....
Frederic R. Morgenthaler
Chairman, Department Committee on Graduate Theses

ELÈCTROMAGNETIC WAVE PROPAGATION IN A MAGNETIZED LABORATORY PLASMA

by

Michael Joseph Rowlands

Submitted to the Department of Electrical Engineering and Computer Science
on May 22, 1998, in partial fulfillment of the
requirements for the degrees of
Master of Engineering
and
Bachelor of Science

Abstract

The Versatile Toroidal Facility (VTF) is a torus of 1 m major radius used to simulate ionospheric plasmas. It is located in the Plasma Science and Fusion Center at MIT and is supervised by Min-Chang Lee. Plasma is formed in the vacuum chamber by two mechanisms: electron emission and microwave resonance heating. The plasma species, hydrogen or argon, is leaked into the chamber at low pressure. A 0.001 tesla uniform vertical field is added to the 0.08 tesla toroidal field to yield a helical magnetic field that guides the electron beams along their path. In the ionosphere, electromagnetic waves below the electron cyclotron frequency, propagating along the earth's magnetic field are called whistler waves. Usually excited by lightning, they are ducted along the earth's magnetic field by volumes of increased plasma density. Waves that are not ducted lose their energy, disperse and are not detected. However, according to Robert Helliwell's theory [1], they are only ducted up to half the electron cyclotron frequency. Rocket experiments have confirmed this theory [2]. In VTF, the electron beams excite whistler waves along the helical magnetic field in the chamber, much like lightning in the atmosphere. Under certain plasma conditions, like lower plasma density, and higher magnetic field, the measured cutoff frequency is closer to ionospheric results. Yet, under many other conditions in the chamber, whistler waves are detected all the way up to the electron cyclotron frequency. This project focuses on the investigation of electromagnetic waves in the VTF chamber in order to understand better this discrepancy. Primarily, the cutoff frequency for these waves in VTF plasma is examined through experiments, theory and computational analysis. An adapted theory is developed to help explain electromagnetic wave propagation in the VTF chamber.

Thesis Supervisor: Min-Chang Lee
Title: Head of Ionospheric Plasma Research Group

Acknowledgments

First and foremost I would like to thank my advisor, Min-Chang Lee. His support and guidance in my years at MIT has been extremely helpful. I appreciate his encouragement in all my endeavors at VTF. He has given me advice about summer programs and has made it possible for me to attend several conferences, including URSI (Union of Radio Science International) and APS (American Physical Society). He has always been available when I had questions or wanted to discuss research with him. He has made my research experience at MIT a pleasant one.

I would also especially like to thank one of my colleagues at VTF, Ryan Riddolls. His tireless, outstanding work at VTF has saved me months of time on my thesis. He keeps the machine running by fixing anything that is broken. He helps me whenever I need it and answers my questions. He does all this on top of working on his own projects. He does so much more than he has to, his dedication and interest in VTF is a great example to me. I will miss working with him.

In addition, I would also like to thank the other students at VTF with whom I have worked: Nathan Dalrymple, Mike Starks, Shaun Meredith, Dan Moriarty, Kevin O'Donnell, Piotr Jastrzebski and Allen Chen. The probes they helped build have been invaluable to me. The things I have learned from them have been beneficial at lab and in life.

In addition, I wish to acknowledge all the people who helped construct the VTF machine. I have not worked with many of them, nor will I list all of them here, but I do appreciate their efforts. Without the work at VTF of all those before me, my research would not be possible.

Lastly, my work was supported by funding from AFOSR (Air Force Office of Scientific Research) and NSF (National Science Foundation). Their financial support of and interest in plasma studies at VTF has made me grateful.

Contents

List of Figures

Chapter 1

Introduction

Whistler waves have intrigued scientists for more than half a century. These electromagnetic waves propagating along the earth's magnetic field gained notoriety during World War I. While listening for enemy radio signals, soldiers often heard a sound, for a few seconds, descending in pitch. Radio signals were affected and sometimes rendered undecipherable during those whistles. Researchers have been studying whistler waves ever since.

Whistler waves are defined as right hand circularly polarized electromagnetic waves propagating at small angles to the magnetic field in a magnetized plasma with frequencies below the electron cyclotron frequency. Electromagnetic waves of this type have a dispersion relation that shows that high frequency waves travel faster in the plasma than low frequency waves. The explanation of whistler wave observations, on the earth's surface, involves a point source and a fixed observer. The source generates a pulse of broad spectrum radiation. The highest frequency waves from the pulse reach the observer first; the lowest frequency waves reach the observer last. Thus, the observer measures waves that continuously decrease in frequency until the pulse is finished. This describes the aforementioned phenomenon discovered during WWI. The point source of radiation was a bolt of lightning; while the fixed observer was a soldier with a radio receiver that converted electromagnetic signals to sound waves.

Today, understanding plasmas and plasma waves continues to have applications

to communications. The interaction of electromagnetic signals with the atmosphere, (the region from 0–100 kilometers altitude), and the ionosphere (the region from 100–600 kilometers altitude), is significant. With the expansion of wireless and satellite communications, the study of the earth's ionospheric plasma has become a more important part of world scientific research.

1.1 Motivation

In a magnetized plasma, whistler waves have some cutoff frequency above which they do not propagate. The reason is that the direction of wave propagation is not identical to the direction of energy travel. For some frequencies and propagation angles with respect to magnetic field, the ray-path oscillates around the direction of the magnetic field. Under these conditions, the wave is said to be ducted. For other frequencies and propagation angles, the ray-path points away from the magnetic field and becomes perpendicular to the field. When this happens, the wave is not ducted. If the observer is several mean free paths away from the whistler wave source, only ducted waves are measured. According to ionospheric wave ducting theory [3], in areas of increased plasma density along a magnetic field line, whistler waves are only ducted up to half the electron cyclotron frequency. Field and rocket experiments have confirmed this result. In VTF, the radial plasma density profile is basically a single crest. Thus, VTF closely models enhanced plasma density along geomagnetic field lines in the ionosphere. However, whistler waves in VTF have been detected all the way up to the electron cyclotron frequency. This discrepancy between lab results and theory has been investigated with the goals of describing and understanding the generation and propagation of high frequency electromagnetic waves in VTF plasmas. In order to do this, research has focused on experimental data of electromagnetic waves in VTF.

1.2 Outline

To describe this project, the VTF machine must first be detailed. Chapter two discuss the hardware used to form plasmas and collect data. The various plasmas sources and diagnostic devices will be specified. The design and construction of the loop probe used to measure electromagnetic waves will be recounted. Once the VTF machine is explained, the theory behind the experiments will be given. Chapter three will cover the theoretical analysis of whistler waves. The derivation of cutoff frequency along geomagnetic field lines will be shown. An adapted theory to describe VTF ducting will relate ionospheric conditions to those of VTF. After these plasma physics calculations, experimental results will be presented. Chapter four will show data concerning electromagnetic waves in VTF. The data will be explained and compared with theory. Detected power densities will be cross-checked with calculations of generated power. To summarize, in chapter five the conclusions of the project will be accounted and future experiments will be recommended.

Chapter 2

The Versatile Toroidal Facility

The construction of the Versatile Toroidal Facility, VTF, was begun in 1989. The majority of its construction was finished in 1991. Plasma was first formed in the VTF chamber in January of that year. Many of the construction materials were made available from discontinued fusion programs. For instance, the toroidal field magnets came from Oak Ridge National Laboratory and the electron beam power supplies came from the MIT Plasma Fusion Center's TARA Tandem Mirror machine. Much of the initial construction of the machine was done by undergraduates through the Undergraduate Research Opportunities Program (UROP) sponsored by the MIT UROP office and the Air Force Office of Scientific Research. Over twenty-five undergraduate and graduates students helped design and build the thirty-ton device.

The major parts of VTF are the vacuum chamber, the power supplies, the plasma sources, the diagnostic instruments, and the data acquisition and control system. Plasma is formed in the vacuum chamber after leaking in a small amount of gas, and activating one of the plasma sources. The power supplies provide the voltages and currents necessary to create the magnetic field in the chamber and run the plasma sources. Measurements come from the power supplies or from probes inserted into the plasma. These measurements are digitized and sent to a computer in the control room which stores them to disk.

2.1 The Vacuum Chamber

The VTF vacuum chamber is a toroidal shape with rectangular cross section. It has a major radius of about 1 m and is made of 3/4-inch thick stainless steel. There are 16 ports on the machine, spaced 20 degrees apart. There are no ports at 0 and 180 degrees because of the seam between the two halves of the chamber. Figure 2-1 shows a schematic. Two pumps keep the chamber at a base pressure on the order of 10^{-7} Torr. Basically, a turbomolecular pump is in series with a roughing pump. The turbo pump is connected to the chamber and the roughing pump is located between the turbo pump and the outside air. A large, flat piece of metal serves as a gate valve between the chamber and the turbo pump. It slides into the opening between them to seal off the chamber from the pumping system. The pump stand is located at 200 degrees.

2.2 The Power Supplies

The microwave generator, the electron emitter filaments, the toroidal field and the vertical field each use several kilowatts of power during operation. Multiple supplies generate the necessary power for these devices.

Three kilowatts of power are delivered to the 2.45 GHz microwave source by a Gerling Labs power supply which plugs into the wall. The emitters are powered by voltage and current controlled supplies in the lower level of the cell. Six of these have been inherited from TARA. There are two parts to each emitter supply: the filament supply and the arc supply. The inputs to these parts are 480 volt lines. The filament supplies are six pulse, phase-controlled primaries of 480 volts transformed down to twenty volts, full-wave rectified, and filtered to reduce ripple. The arc supplies have one six pulse phase-controlled primary feeding delta-delta and delta-y transformers to produce a twelve pulse output at 360 volts. Current is regulated by a bank of parallel resistors between the supply output and the emitter filament. The resistors are switched in and out of the circuit by power transistors. If more current in the

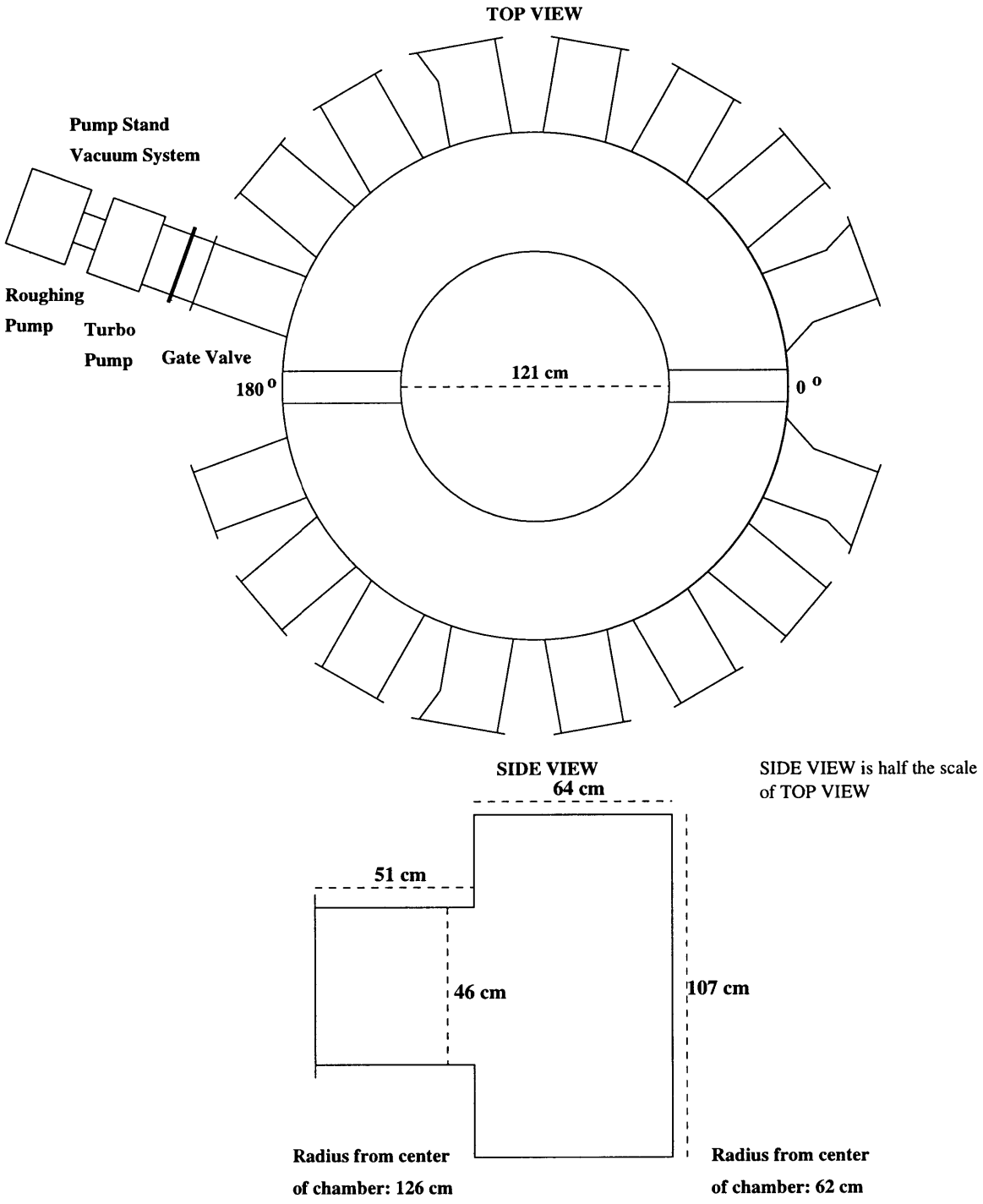

Figure 2-1: Top and side views of the VTF vacuum chamber

plasma is desired, more transistors turn on, more parallel resistors are added and the total resistance decreases. If less current is desired, some transistors are switched off. The vertical magnetic field coils also use this type of supply. Helmholz coils generate a field of ten gauss per kiloamp using the filament supply of another emitter supply. Around 1000 amps is run through the coils during a plasma experiment, creating a uniform magnetic field straight up and down in the plasma chamber.

In order to maintain a steady-state plasma density, a substantial toroidal magnetic field is necessary to produce and confine plasma. The configuration of the magnet coils creates a field strength that is inversely proportional to radius. A toroidal field of 800 gauss is typical at a radius of 100 centimeters, around the peak beam plasma density. Eighteen coils of four turns each are wrapped around the chamber. Between 4,000 and 10,000 amps are run through the seventy-two turns to produce the toroidal field. Two power converters generate this current. The input to the converters is 480 volt, three phase power. Six silicon controlled rectifiers (SCRs) full wave rectify the input to a DC voltage. The output current is set from the control room and is regulated by changing the firing angle of the SCRs [6].

2.3 The Plasma Sources

The base pressure in the vacuum chamber is around 5×10^{-7} Torr. Hydrogen or argon gas is leaked at about 2×10^{-4} Torr. Valve regulators control the flow of gas between the metal tanks and the vacuum chamber. Once the gas is in the chamber, there are two ways to form a plasma: firing electron beams or injecting microwaves (Figure 2-2). One or both of these are used to create the desired conditions for an experiment.

2.3.1 Electron Emitter Filaments

Streams of electrons are generated and accelerated along the magnetic field in the chamber. These high speed electrons from the filament collide with neutral gas atoms and ionize them, forming a plasma. There are two filaments on the bottom of the plasma chamber which are spaced 180 degrees apart, at 60 and 240 degrees. A filament

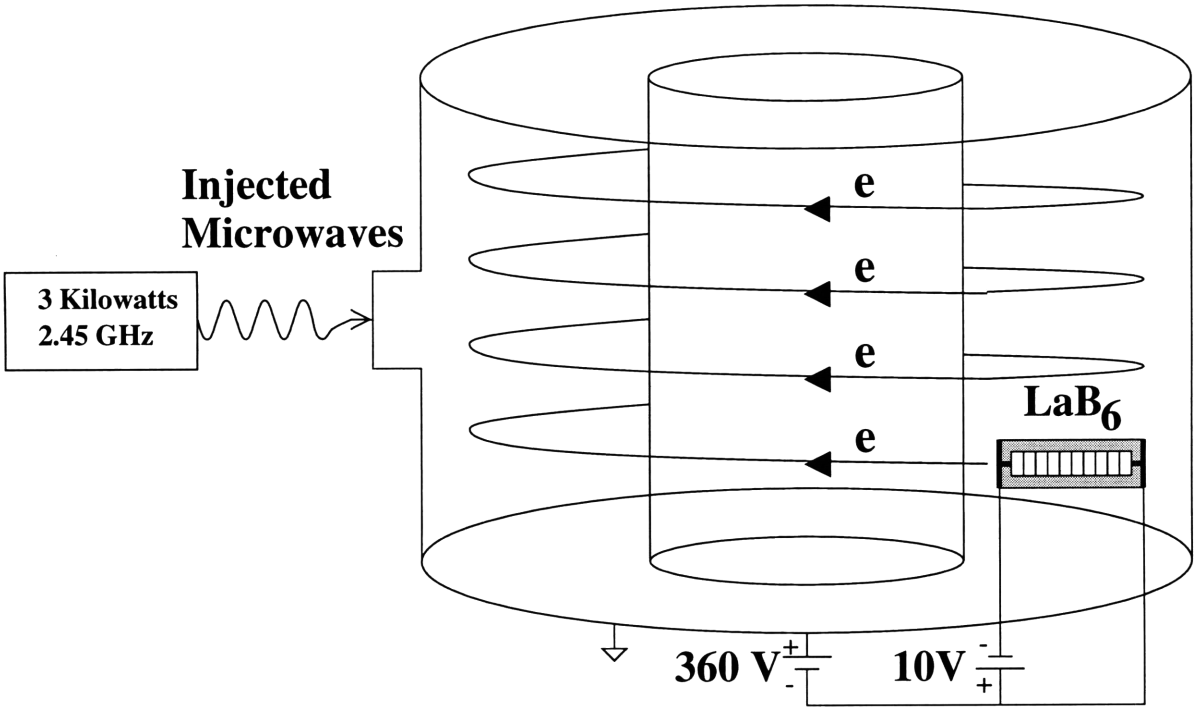

Figure 2-2: Schematic of beam and microwave plasma sources

consists of LaB_6 (lanthanum hexaboride) rings around a carbon rod. The carbon rod is then fastened to a carbon plate at both ends. On the back side of the filament (the side opposite the direction of emitted electrons) there are two steel plates. These backplates direct the beam clockwise. To produce a beam, the lanthanum hexaboride rings are heated and subsequently biased with a negative voltage. Electrons are emitted from the LaB_6 under these conditions and are accelerated along the helical magnetic field. The rings are heated to 1600 degrees Celsius by running a current through the carbon rod holding the rings, for sixty seconds. Then the filament is biased at -360 volts for the duration of the plasma shot, usually three seconds. Each beam can produce a beam current of up to 200 amps. Common beam currents are 50 amps from each beam, yielding a peak plasma density of about 10^{17} ions/m^3. Figure 2-3 shows a typical density profile for beam plasmas and the background magnetic field strength. [4]

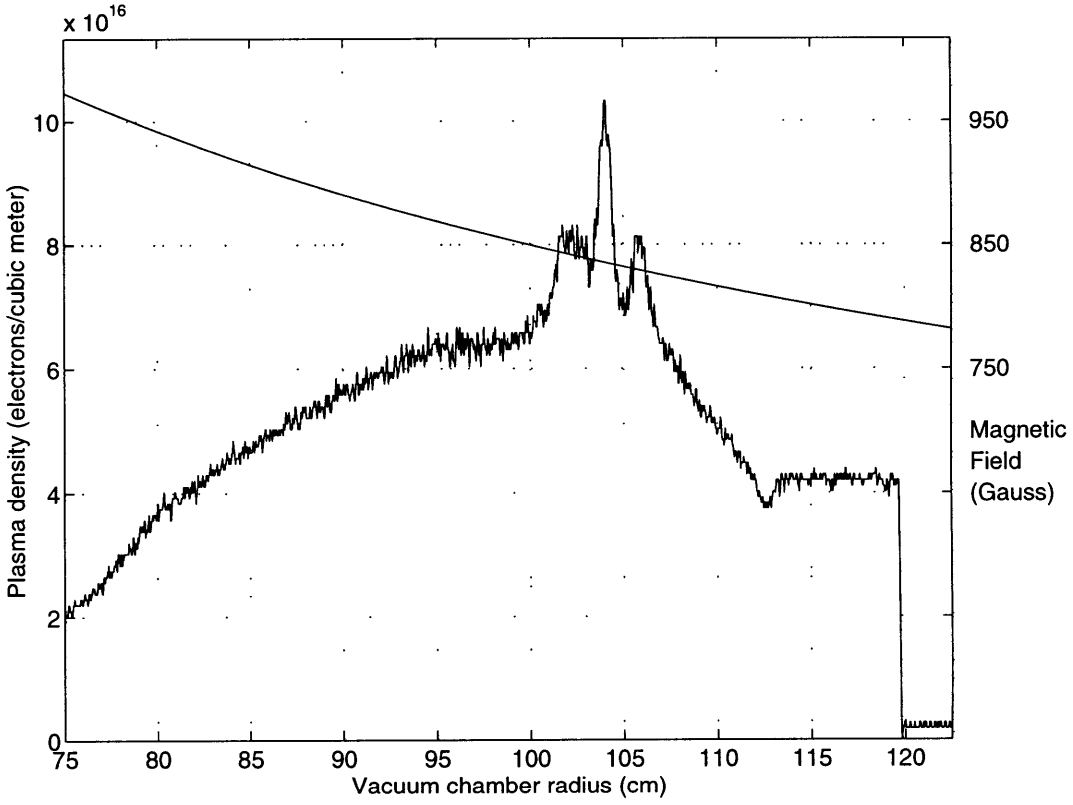

Figure 2-3: Plasma density and toroidal field magnitude for a two beam shot

2.3.2 Microwave Source

The second way of producing a plasma uses a three kilowatt, 2.45 GHz microwave. The microwave source is located at 40 degrees. Microwaves are injected radially into the chamber. When the 2.45 GHz waves are in resonance with the electrons gyrating in the background magnetic field, some electrons gain enough energy to ionize the gas. This electron cyclotron resonance heating, ECRH, occurs around the location that the electron cyclotron frequency matches the injected wave frequency. Generally, ECRH plasmas have a peak density on the order of 10^{16} ions/m^3. Figure 2-4 shows a typical density profile for microwave plasmas and the background magnetic field strength.

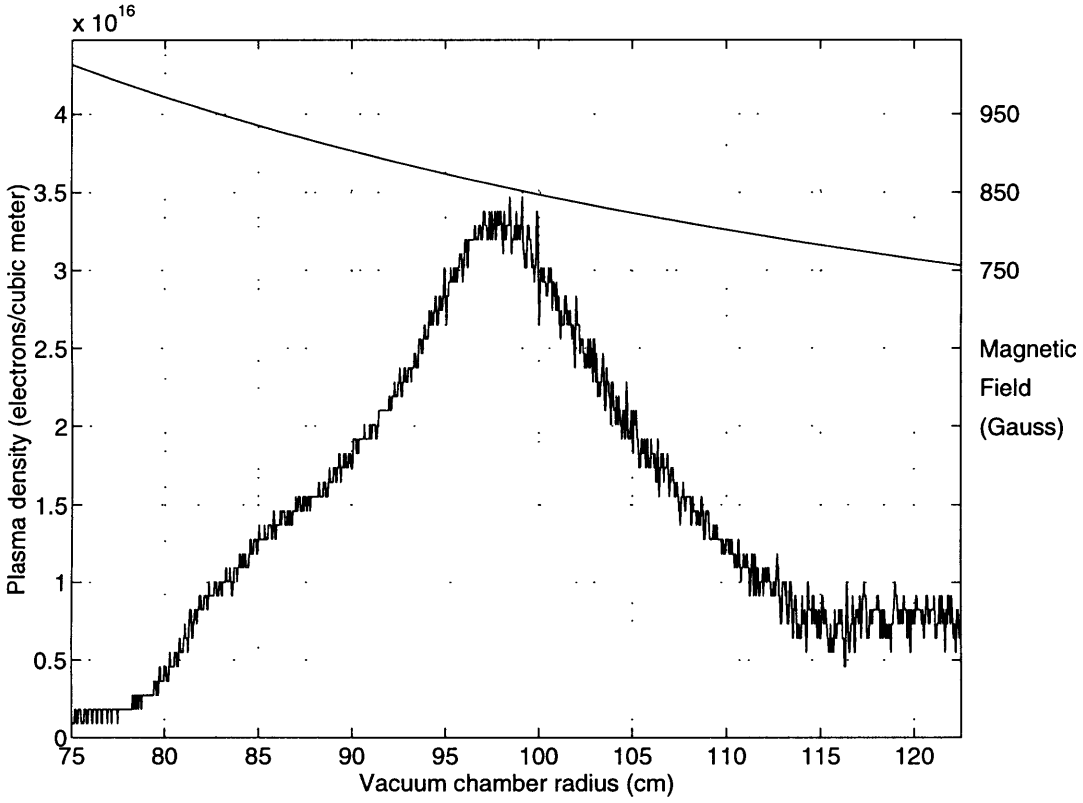

Figure 2-4: Plasma density and toroidal field magnitude for an ECRH shot

2.4 The Diagnostic Instruments

There are five probes inserted into the plasma chamber. Each probe has one or more tips that take measurements of the plasma; these include a dipole probe, a radially scanning probe, two loop probes and a gridded energy analyzer (Figure 2-5). The probes are used to measure a variety of plasma parameters and waves which will be detailed later. There is also another set of measurements digitized from wires connected to the power supplies used to run the machine. This engineering information, like toroidal field current, beam voltage, filament current, is used to make sure the machine is working properly and get a rough idea of plasma conditions.

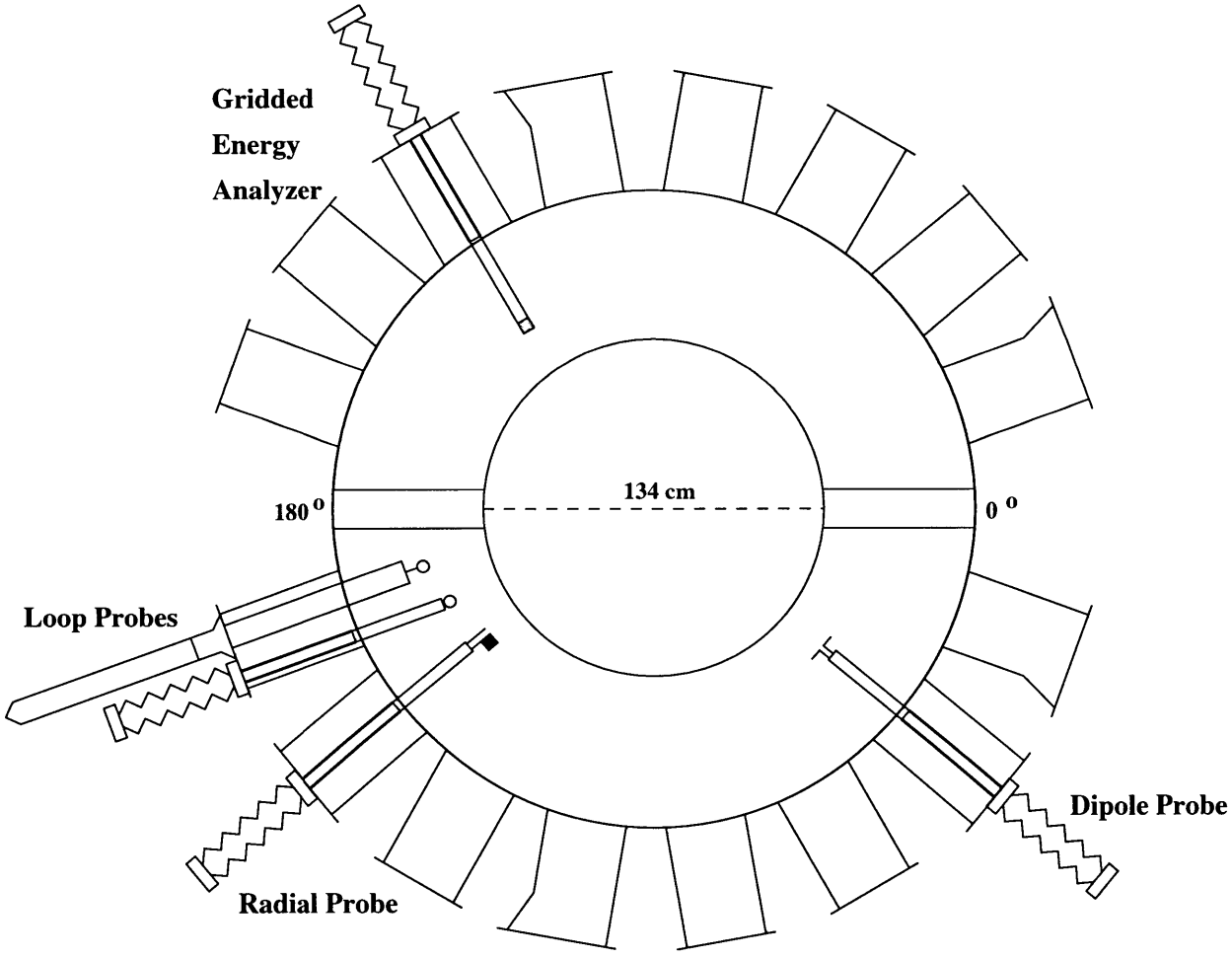

Figure 2-5: Overhead view of chamber and inserted probes

2.4.1 Dipole Probe

The dipole probe has two wires protruding in opposite directions. It measures voltage differences between those two wires. Fluctuations in the megahertz and gigahertz range can be detected. Electrostatic waves propagating parallel to the dipole are preferentially detected. The probe is located at 40 degrees in the chamber. Electric fields of electromagnetic waves can also be detected by the dipole. A rotating feedthrough allows the dipole orientation to be changed during a single plasma shot.

2.4.2 Radial Probe

The radial probe has three tips and is located at 140 degrees. Its three tips are a single wire, a dipole and a wire with a square of metal at the end, known as the flag tip.

The single wire measures potential. Electrostatic waves, electromagnetic waves and plasma potential can be measured by allowing the probe tip to float and measuring its voltage with respect to ground.

Data from the Langmuir probe (the flag tip) is used to measure electron temperature and plasma density using methods described by Langmuir. By biasing the flag tip and sweeping its voltage around the floating plasma potential, electron temperature can be determined. Depending on whether the sweeping voltage is above or below the plasma potential, electrons are either attracted or repelled, respectively. Both probe current and probe voltage are measured and digitized. This voltage vs. current characteristic is used to calculate the electron temperature. [5] Plasma density is found by biasing the probe at a DC voltage well below the plasma potential; the current drawn from the plasma is proportional to density. A Langmuir probe box is connected to the flag tip in order to make these measurements. It biases the tip to a DC or sweeping voltage, reads the current drawn through the tip from the plasma, and outputs its voltage and current measurements to the data acquisition system.

The fixed-angle dipole probe is used in the same manner as the rotating dipole probe. However, the probe has a controlled motor which moves it radially. Thus, all

three probe tips can be moved along the radius during a single plasma shot. Given that plasma conditions are stable during the shot, the radial probe allows plasma density vs. radius profiles to be taken.

2.4.3 Loop Probes

Loop probes were the main diagnostic instruments for this project. They are located side by side at 160 degrees. The probes have tips that are either one or two loops of wire. They detect a changing magnetic field perpendicular to the loops, inducing a voltage across the loops which can be measured using a spectrum analyzer. Since the only changing magnetic fields at gigahertz frequencies are electromagnetic waves propagating in the plasma, the loop probe diagnostics give a direct measurement of whistler waves. Electromagnetic waves in the megahertz and gigahertz range are detected with these probes. One probe uses a rotatable vacuum seal. The other uses vacuum bellows and easily moves in and out of the chamber. This probe has loops whose normal is radial in the chamber, while the rotatable probe has a loop whose normal can be rotated from parallel to vertical with respect to the toroidal field.

Radial Loop Probe

Figure 2-6 shows the radial loop probe and its components. The radial loop probe has two loops as its tip. Facing parallel to the walls of the chamber, the loop tip is oriented so that the normal to the loops is exactly radial. Electromagnetic waves traveling parallel to the toroidal field will have a magnetic field perpendicular to the loop tip, inducing a voltage across the tip. The two ends of the loop tip are each soldered to the inner conductor of a separate 50 Ω copper semirigid co-axial cable. The outer conductors are connected and grounded at the tip and at the vacuum feedthrough. Covering it are several layers of ceramic paint which prevents electrons from contacting the tip. Then a ceramic pipe covers the co-axial cable from the tip to the steel pipe. Set screws connect the ceramic pipe to a slightly larger steel pipe which is welded to a double-sided flange at the back of the probe. Bolted to the

double-sided flange are the SMA feedthrough on one side and the end of the bellows on the other. The feedthrough must hold vacuum since it has the vacuum chamber on one side and ambient air on the other. The bellows goes between the double flange and the half nipple on the vacuum chamber port. The probe tip is fixed with respect to the double flange; it is basically at the end of the rigid pipe welded to the flange. In order to move the probe radially, the bellows must stretch and compress. The limits of the bellows length for the loop probe are three inches minimum and twenty-two inches maximum, so it has nineteen inches of throw. Therefore, the probe can reach from a radius of 85 cm to a radius of 133 cm. It can be moved between shots. It is desired that the loop probe only detect magnetic fields, so electrostatic

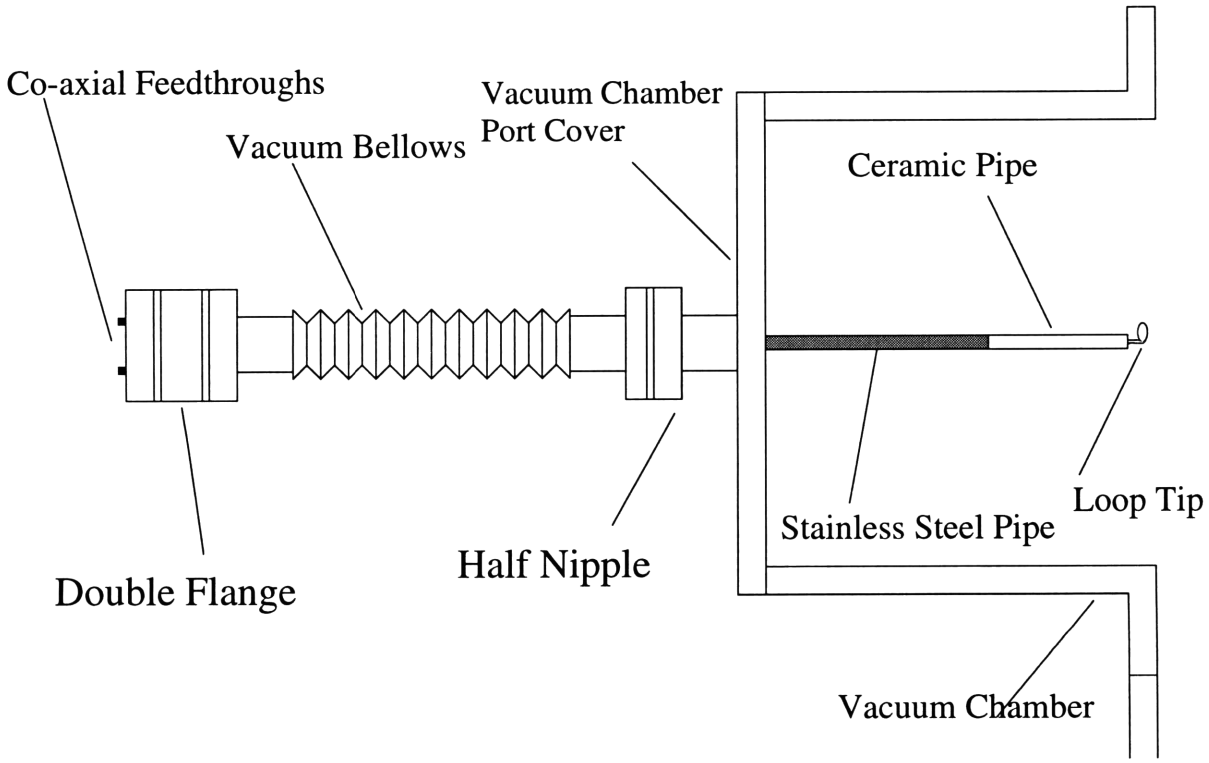

Figure 2-6: Side view of radial loop probe

signals must be eliminated. Although no insulation is perfect, ceramic paint and ceramic pipe are sufficient to prevent many electrons from hitting the probe tip. However, electric field signals also have to be eliminated. The induced voltage across the loop is between the inner conductors of the connectors on the SMA feedthrough. An H-183 M/Acom microwave subtractor takes the two signals, finds the difference

between them, and sends the resulting signal to the spectrum analyzer. Since the outer conductors shield electric fields and are grounded, the signal detected is purely from changing magnetic fields normal to the loop. Therefore, any electrostatic signals are shielded or subtracted out.

Rotatable Loop Probe

The rotatable loop probe is a long pipe with 50 ohm co-axial cable inside it (Figure 2-7). At the end inside the chamber, a single wire loop is soldered to the cable. The rotatable vacuum seal is provided by two rubber o-rings which slide over the metal pipe. The pipe can slide in and out and rotate during vacuum. This is useful because the loop tip orientation can be changed during experiments. Since the tip preferentially detects electromagnetic waves propagating in the plane of the loop, the rotatable loop probe gives some idea of the direction of wave propagation.

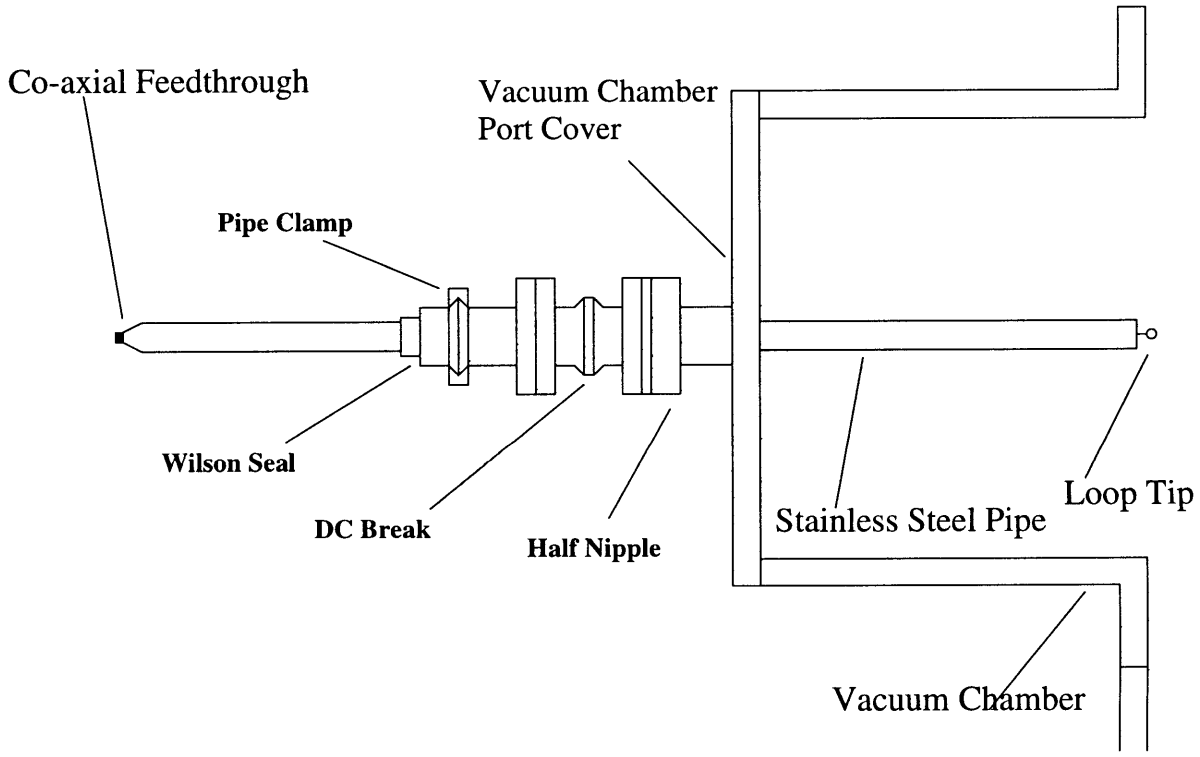

Figure 2-7: Side view of rotatable loop probe

2.5 The Data Acquisition and Control System

In order to form a plasma in VTF, several things must happen. The chamber must be at a low enough pressure and hydrogen or argon gas must be leaked in. The power supplies must have all their circuit breakers turned on. Every safety switch must be closed, i.e. all doors in the gate around the cell must be closed, the water coolant must be flowing at a sufficiently high rate. The control computer must detect that all these conditions are met when the go button is pressed for the shot to start. A diagram of the data acquisition and control system is shown in Figure 2-8. Each object will be further discussed in the following paragraph.

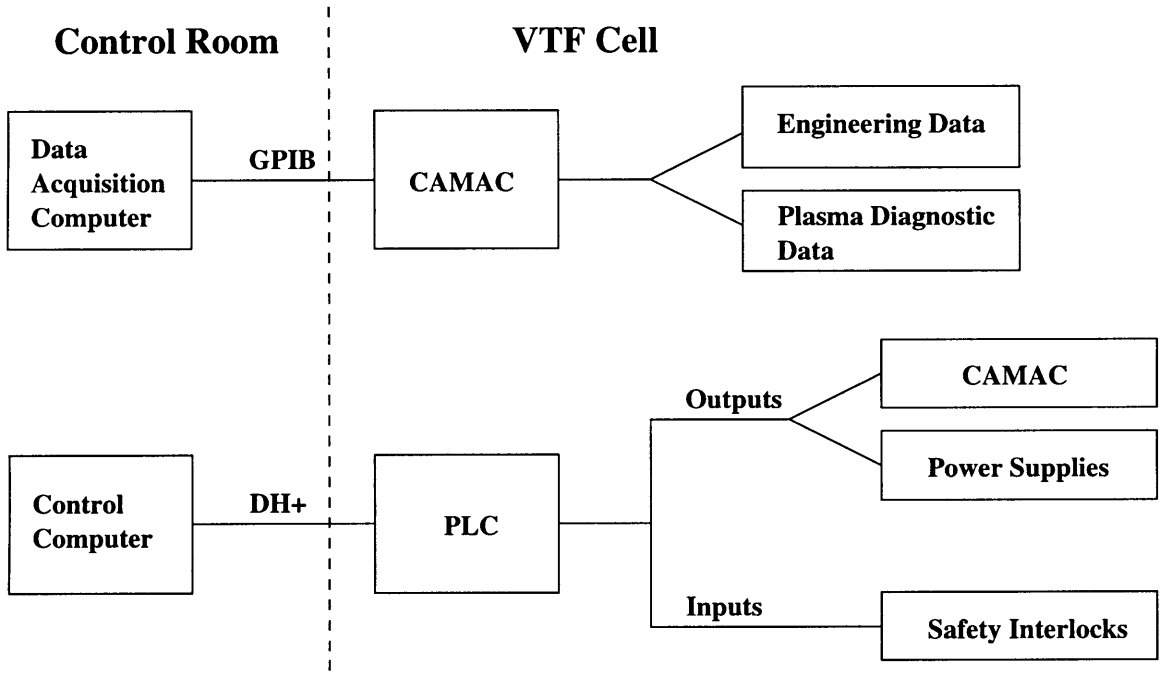

Figure 2-8: Block diagram of data acquisition and control system

The control computer sends signals out to the a large crate in the cell. This computer sits in the control room and has a Paragon interface. Paragon allows the user to input the times when instruments will turn on and off. It also lets the user enter the desired voltages and currents of the power supplies. All the power supplies are controlled in this way: the operator types in the start time, end time and amount of current and/or voltage desired, Paragon runs the programmable logic controller (PLC) software, and the PLC software communicates with the cabinet in the cell.

In the cell cabinet there are CAMAC cards, PLC cards, and fiber optic transmitters and receivers. The PLC in the cell receives the signals from the control computer. It then sends out signals to the CAMAC, to relays or to fiber optic transmitters. The CAMAC is triggered by a signal from the PLC to start taking data. Several instruments are turned on and off by relays and require signals from the PLC. The fiber optic transmitters control the power supplies by signalling when to turn on and off and what voltages and currents to produce [6].

Once the plasma is formed, data is stored in the CAMAC memory modules. The data comes from CAMAC digitizers which are basically analog to digital converters. The analog voltages entering the digitizers come from several sources. Engineering data from the power supplies in the lower level of the cell are input to fiber optic receivers, which, in turn, output a voltage to a digitizer. An isolation amplifier reads the voltage across the toroidal field coils, amplifies it and outputs to a digitizer channel. Probe current and voltage measurements are sent from the Langmuir probe box to the CAMAC. Spectrum analyzer traces are often digitized as well. As soon as the digitizers receive these signals, they store the data in the memory modules. The data acquisition computer is sent the data via a GPIB communications interface. There are currently two digitizer modules that take data. One digitizes at 200 Hz, the other at 10 KHz. A program on the data acquisition computer sets the digitizer rates before the shot, reads out the data in the CAMAC memory modules when accessed, then stores the data to files on disk. Once the data files are on disk, they are loaded, processed and viewed using MATLAB. Usually data is simply converted to a voltage or current and plotted, but sometimes digital filtering or curve-fitting is desired.

All the parts of the data acquisition and control systems combine to give the VTF researcher many ways to create, perturb, and observe plasma processes.

Chapter 3

Theoretical Analysis

3.1 Whister Wave Ducting in a Crest

The propagation characteristics of electromagnetic waves in a magnetized plasma have been studied. Using the dielectric tensor for a plasma, the dispersion relation for electromagnetic waves can be found. The dispersion relation is a function of angle of propagation with respect to the background magnetic field. [7] Also, a magnetized plasma is anisotropic so a wave's direction of propagation through it may be different than its direction of energy flow. The dispersion relation is dependent on plasma frequency and therefore dependent on plasma density as well. Thus, changes in density do affect wave propagation. All of these factors in the dispersion relation: direction of propagation, direction of energy flow, and plasma density, combine to show that in a varying density profile, under certain conditions, energy flow and direction of propagation diverge and become perpendicular. When this happens, no component of wave energy is in the direction of wave propagation and the wave ceases to propagate. If direction of propagation and energy flow remain at an acute angle to each other and the wave energy stays in the plasma then the wave is said to be ducted.

Wave ducting analysis is done via a Snell's law construction, i.e. the component of a $\vec{k}$ tangential to a boundary is equal on both sides of the boundary. Suppose that the plasma medium is divided into thin laminae parallel to the background magnetic

field. Within each lamina, the plasma is considered to be homogeneous and the ray path angle and propagation angle of the wave are constant. At the boundary between two laminae, Snell's law is used to find the ray path and propagation direction of the wave in the next lamina. This analysis assumes that the plasma parameters vary slowly with respect to the laminal thickness and the perpendicular component of the whistler wavelength. If it is found, after applying Snell's law, that a whistler wave packet can become trapped in a volume consisting of a finite number of contiguous laminae, then the trapping structure is referred to as a duct.

From the dielectric tensor of magnetized plasma media the cold plasma dispersion relation for whistler waves is as follows:

$$\mu^2 = 1 - \frac{X}{1 - iZ - \frac{\sin^2\theta}{2\Lambda^2(1-X-iZ)} \pm \frac{1}{1-X-iZ}\left[\frac{\sin^4\theta}{4\Lambda^4} + \frac{\cos^2\theta}{\Lambda^2}(1-X-iZ)^2\right]^{\frac{1}{2}}} \tag{3.1}$$

μ = index of refraction

ω_o = whistler wave frequency

ω_{ce} = electron cyclotron frequency

ω_{pe} = plasma frequency

θ = angle between wave normal and magnetic field

ν = electron-neutral collision frequency

$$\Lambda = \frac{\omega_o}{\omega_{ce}} \tag{3.2}$$

$$X = \frac{\omega_{pe}^2}{\omega_o^2} \tag{3.3}$$

$$Z = \frac{\nu}{\omega_o} \tag{3.4}$$

Given ionospheric conditions:

$$\omega_o \gg \nu$$

$$\sin^2\theta \ll 2\Lambda^2(1-X)$$

$$\omega_{pe} \gg \omega_{ce}$$

The dispersion relation simplifies to:

$$\mu^2 = \frac{-\frac{\omega_{pe}^2}{\omega_{ce}^2}}{\Lambda^2\left(1-\frac{\cos\theta}{\Lambda}\right)} \tag{3.5}$$

Ray path of a wave denotes direction of energy flow in a medium. The index of refraction surface is the plot of a function where y= $|\mu(\theta)\cos\theta|$ and x=$|\mu(\theta)\sin\theta|$. Ray path is perpendicular to the index of refraction surface. In an anisotropic medium, like a magnetized plasma, ray-path and propagation direction of a wave may not be the same. Let α the angle between the ray path and wavenormal of a whistler wave and can be calculated using the Snell's law construction mentioned earlier. This is shown in Figure 3-1. Index of refraction is plotted in terms of θ at a fixed location in the plasma so that Λ and ω_{pe}^2 are constant. The k-vector of the wave is the line between the origin and the point on the curve $\mu(\theta)\cos\theta$. The ray path is the line perpendicular to the index of refraction surface. When α reaches 90^o, the electromagnetic wave no longer propagates in the anisotropic medium because no component of the wave's energy is in the direction that the wave fronts are traveling [1] (Figure 3-2). The expression relating α to the index of refraction is:

$$\tan\alpha = \frac{1}{\mu}\frac{d\mu}{d\theta} \tag{3.6}$$

Using 3.5, the equation for α is:

$$\alpha = \tan^{-1}\left(\frac{\sin\theta}{2[\cos\theta-\Lambda]}\right) \tag{3.7}$$

For ducting to occur in an area of increased plasma density, ray path must bend toward the enhancement as it tends toward areas of decreased density, and the angle between ray path and k-vector always must be less than ninety degrees (Figure 3-2). In a crest, as wave energy moves away from the density enhancement, density

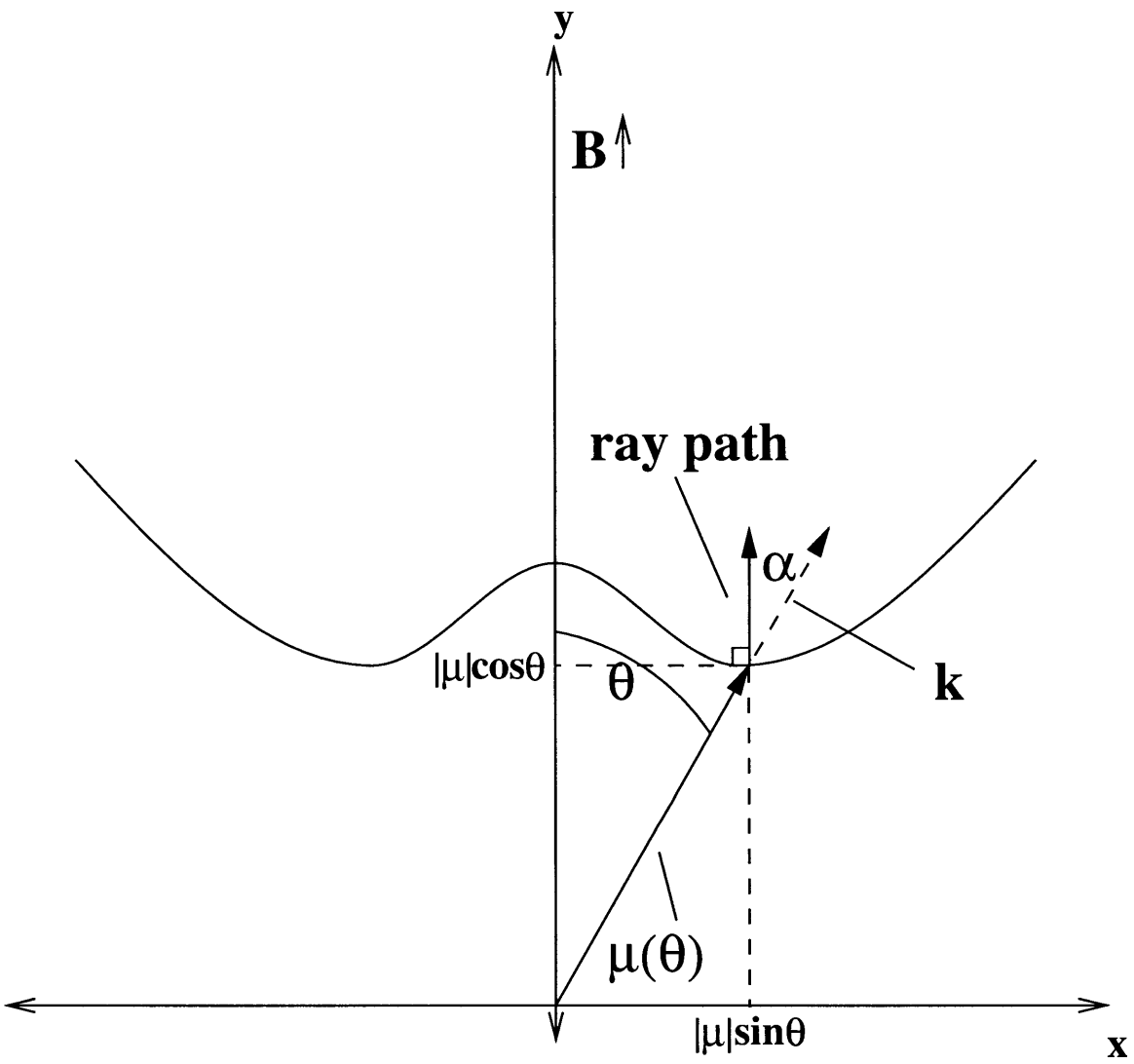

Figure 3-1: Index of refraction and ray path as a function of angle with respect to magnetic field.

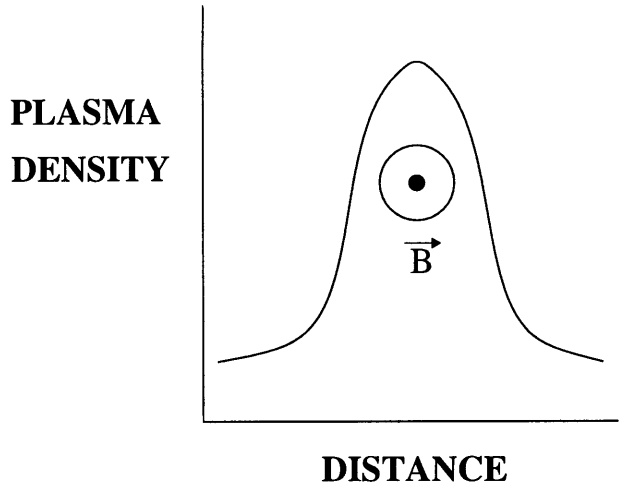

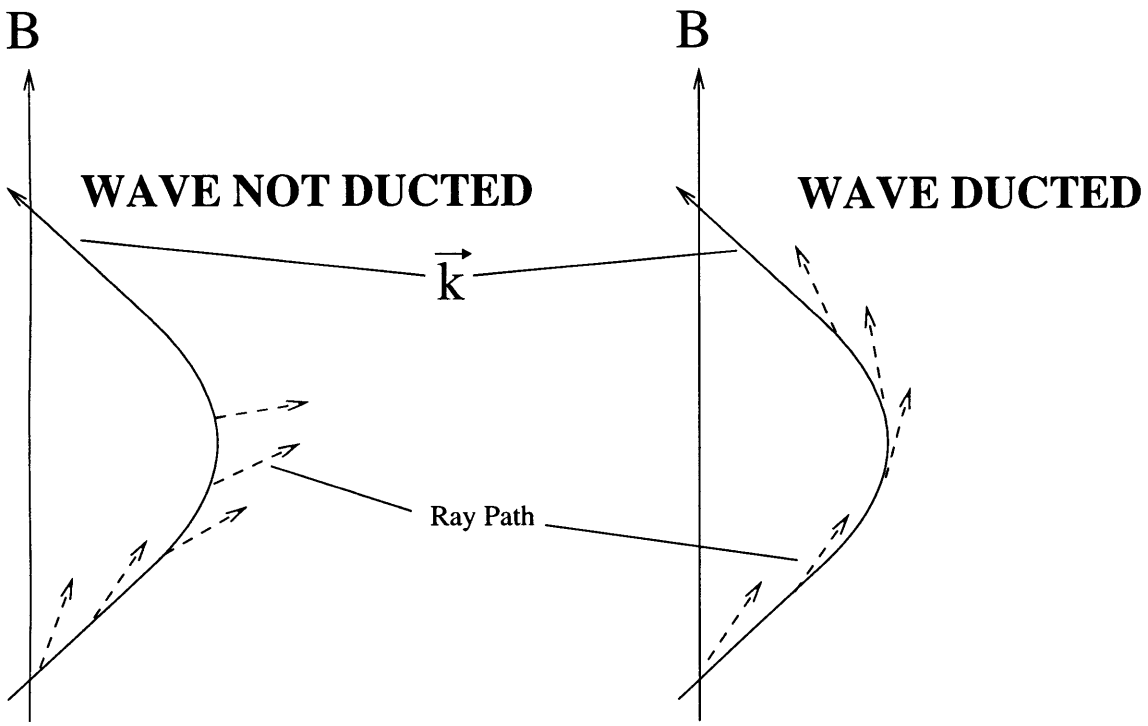

Figure 3-2: Plasma density profile and k-vector path vs. ray path for ducted and non-ducted signals

decreases and thus the magnitude of the index of refraction decreases. When the index of refraction decreases, the propagation angle also decreases because the k-vector always bends toward a higher index of refraction. Furthermore, the ray path angle must decrease as the k-vector decreases or else they become become orthogonal to each other and the wave no longer propagates. However, for ducting to occur, the k-vector and ray path must bend and reverse direction at some point. In terms of angles, the angle of wave propagation with respect to magnetic field is θ and the angle of ray path with respect to magnetic field is $\theta - \alpha$. Therefore, for ducting to occur, as θ increases, $\theta - \alpha$ must increase and index of refraction must increase with increasing plasma density. It can be shown that index of refraction increases with increasing density for $\Lambda < 1$, which is true for all whistler waves. [8] Thus, the ducting conditions reduce to finding when there is a local maximum on the index of refraction surface. From an analysis of the critical points on the index of refraction surface, the only place a local maximum can occur is at $\theta = 0$ (Figure 3-3). Plotting $\theta - \alpha$ vs. θ, in Figure 3-4 and finding Λ where the maximum $\theta - \alpha$ is at $\theta = 0$ yields values of Λ where the index of refraction has a local maximum at $\theta = 0$. Another way of describing the ducting conditions is that $\mu(\theta)\cos(\theta)|_{\theta=0}$ is a local maximum. The values of Λ that satisfy these conditions give cutoff frequencies in a crest. (Figure 3-4)

The highest frequency where ducting can still happen is where $\theta - \alpha$ remains constant as θ increases (Figure 3-3).

Algebraically, the conditions for ducting, in a crest, are as follows:

$$\frac{d(\theta - \alpha)}{d\theta}|_{\theta=0} \geq 0 \tag{3.8}$$

$$1 - \frac{d\alpha}{d\theta}|_{\theta=0} \geq 0 \tag{3.9}$$

$$\frac{d\alpha}{d\theta} = \frac{2(\cos\theta - \Lambda)\cos\theta + 2\sin^2\theta}{4(\cos\theta - \Lambda)^2 + \sin^2\theta} \tag{3.10}$$

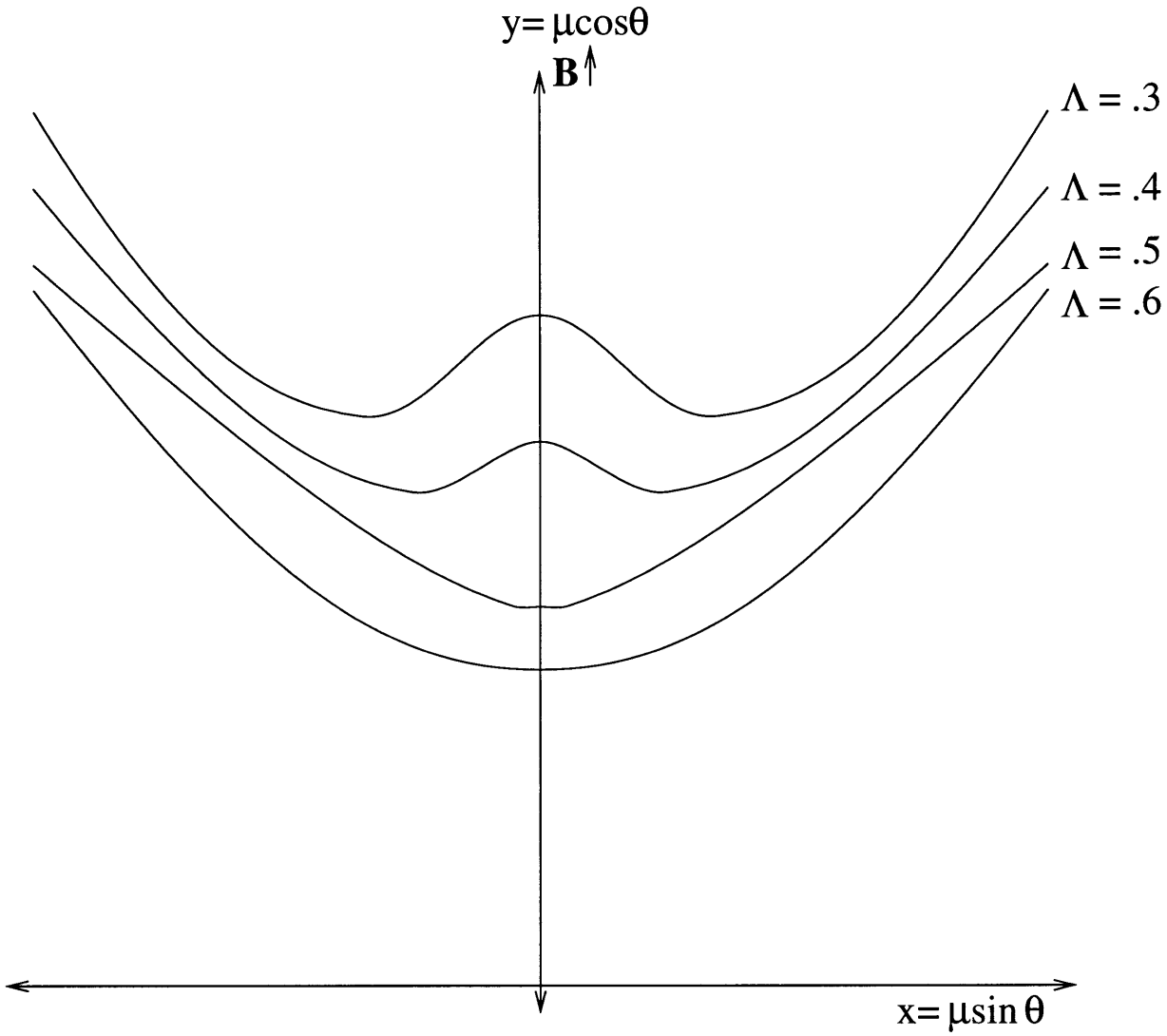

Figure 3-3: Index of refraction profiles for various whistler frequencies; ducting can occur for $\Lambda < .5$

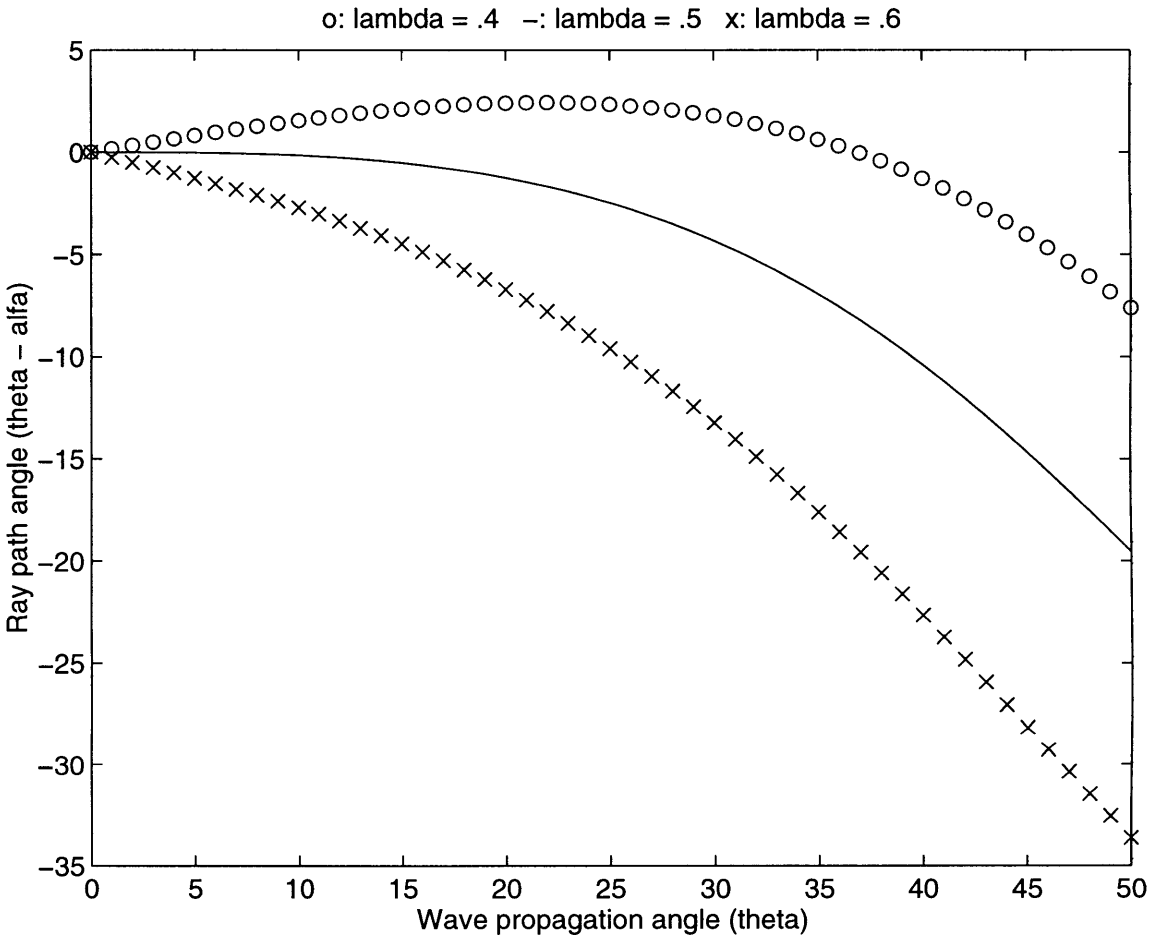

Figure 3-4: Ray path vs. propagation angle for various whistler frequencies

$$\frac{d\alpha}{d\theta}|_{\theta=0} = \frac{1}{2(1-\Lambda)} \tag{3.11}$$

$$1 - \frac{1}{2(1-\Lambda)} = 1 - 2\Lambda = 0, \Lambda = \frac{1}{2} \tag{3.12}$$

It can be seen that the cutoff frequency, $\Lambda \cdot \omega_{ce}$, is half the cyclotron frequency for electromagnetic waves in the ionosphere. In VTF, the approximation that $\omega_{pe} \gg \omega_{ce}$ does not hold. For instance, at a radius of 100 cm, during a beam plasma with 6000 amps of toroidal field current, the plasma density is about 10^{17} ions/m^3. The magnetic field is 0.084 tesla. So ω_{ce} is $1.5\times10^{10}\frac{1}{sec}$ and ω_{pe} is $1.8\times10^{10}\frac{1}{sec}$. Therefore, $\frac{\omega_{pe}^2}{\omega_{ce}^2} = 1.45 \not\gg 1$ and the first term is the index of refraction is not negligible. An adapted theory is necessary to analyze ducting for VTF conditions. Following the same analysis as was done above with ionospheric ducting, but keeping everything except the collisional term in the index of refraction expression:

$$\mu^2 = 1 - \frac{X}{1 - \frac{\sin^2\theta}{2\Lambda^2(1-X)} \pm \frac{1}{1-X}\left[\frac{\sin^4\theta}{4\Lambda^4} + \frac{\cos^2\theta}{\Lambda^2}(1-X)^2\right]^{\frac{1}{2}}} \tag{3.13}$$

Once again, the conditions for ducting are that $\frac{d(\theta-\alpha)}{d\theta}|_{\theta=0} \geq 0$ and that $\mu(\theta)\cos\theta|_{\theta=0}$ is a local maximum.

For simplicity, the index of refraction can be written as:

$$\mu^2 = 1 - \frac{X}{A} \tag{3.14}$$

$$X = \frac{\omega_{pe}^2}{\omega_o^2} \tag{3.15}$$

$$A = 1 - \frac{\sin^2\theta}{2\Lambda^2(1-X)} + \frac{1}{1-X}\left[\frac{\sin^4\theta}{4\Lambda^4} + \frac{\cos^2\theta}{\Lambda^2}(1-X)^2\right]^{\frac{1}{2}} \tag{3.16}$$

In order to find the ducting conditions start with the expression for α:

$$\tan\alpha = \frac{1}{\mu}\frac{d\mu}{d\theta} = \frac{X\frac{dA}{d\theta}}{2A(A-X)} \tag{3.17}$$

$$\frac{dA}{d\theta} = \frac{-\sin\theta\cos}{\Lambda^2(1-X)} + \frac{1}{2(1-X)}\left[\frac{\sin^4\theta}{4\Lambda^4} + \frac{\cos^2\theta(1-X)^2}{\Lambda^2}\right]^{\frac{-1}{2}}\left[\frac{\sin^3\theta\cos\theta}{\Lambda^4} - \frac{2\cos\theta\sin\theta(1-X)^2}{\Lambda^2}\right] \tag{3.18}$$

Calculating the derivative of α with respect to θ:

$$\frac{d\alpha}{d\theta} = \frac{d}{d\theta}\left(\tan^{-1}\left[\frac{X\frac{dA}{d\theta}}{2A(A-X)}\right]\right) \tag{3.19}$$

$$B^2 = \frac{\omega_{pe}^2}{\omega_{ce}^2} = \frac{X}{\Lambda^2} \tag{3.20}$$

$$\frac{d\alpha}{d\theta}|_{\theta=0} = \Lambda\left(\frac{2\Lambda^4}{B^2(B^2-1)} - \frac{4\Lambda^3}{B^2(B^2-1)} - \frac{2\Lambda^2}{B^2} + \frac{5\Lambda}{B^2-1} + \frac{2B^2-3}{B^2}\right) \tag{3.21}$$

The maximum ducting frequency condition becomes:

$$\frac{d(\theta-\alpha)}{d\theta}|_{\theta=0} = 1 - \frac{d\alpha}{d\theta}|_{\theta=0} = 0 \tag{3.22}$$

$$\frac{d\alpha}{d\theta}|_{\theta=0} = 1 \tag{3.23}$$

The equation for Λ in terms of B^2 is:

$$0 = -2\Lambda^5 + 4\Lambda^4 + 2\Lambda^3(B^2-1) - 5B^2\Lambda^2 + \Lambda(B^2-1)(3-2B^2) + B^2(B^2-1) \tag{3.24}$$

Plotted in Figure 3-5 is Λ vs. $\frac{\omega_{pe}}{\omega_{ce}}$. It can be seen from the graph that as plasma frequency becomes large compared to electron cyclotron frequency, the whistler wave cutoff frequency approaches half the cyclotron frequency. This supports the approximations made in the ionospheric ducting analysis. Also, it shows that for plasma frequencies decreasing towards the cyclotron frequency, the whistler wave cutoff decreases. Thus, electromagnetic wave ducting analysis shows that in a crest of plasma

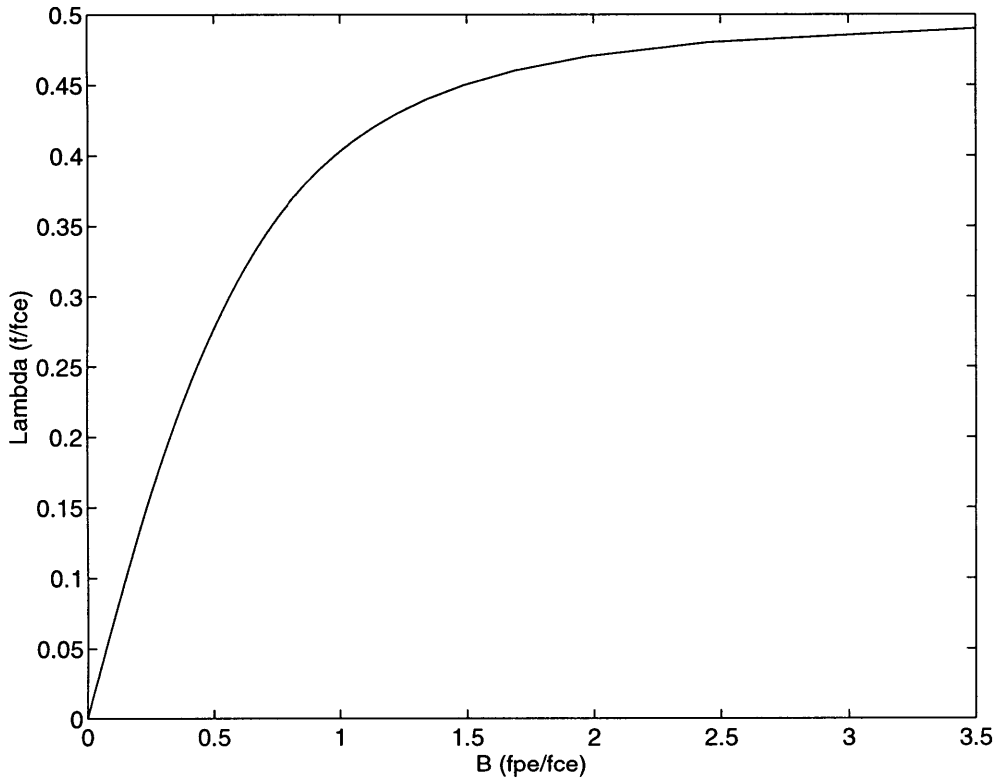

Figure 3-5: Whistler wave cutoff frequency vs. plasma frequency

density, whistler waves cannot be ducted above half the cyclotron frequency. Since waves above half the cyclotron frequency are in fact detected in laboratory experiments, this ducting theory does not fully explain whistler wave propagation in the VTF chamber.

3.2 Whistler Wave Ducting in a Trough

The analysis of whistler wave propagation in an area of decreased plasma density is similar to the analysis discussed previously in this chapter. However, since the magnitude of the index of refraction increases as the wave moves away from the duct, the conditions for ducting change. In a plasma trough, a volume of depleted ionization, ducting will occur if and only if $\frac{d[\mu(\theta)\cos\theta]}{dn} > 0$ in some finite neighborhood of a local minimum of $\mu(\theta)\cos\theta$, where n is the plasma density [8]. It is clear that index of refraction is a strong function of density since it has a term proportional to the local plasma frequency. Thus, as mentioned earlier in this chapter, for whistler wave frequencies, index of refraction goes up with increasing plasma density and down with decreasing plasma density. As a wave leaves the duct, it experiences an increase in plasma density therefore a decrease in index of refraction. In a trough, the line of cutoff frequency is the same as for a crest. It is the line where the critical point in the index of refraction surface, at $\theta = 0$, changes from a local minimum to a local maximum. Qualitatively, it can be seen that for all values of Λ, ducting can occur because a local minimum exists for all values of Λ. (Figure 3-3) The difference is that in a trough, ducting occurs above that frequency, not below. The critical points on the index of refraction surface were already found in the analysis of crest ducting. The results for the ionospheric case are shown in Figure 3-6. Notice that at $\theta > 0$, ducting in a trough can occur below half the cyclotron frequency. However, when $\cos\theta > \Lambda$ the index of refraction for whistler waves becomes imaginary so trough ducting does not occur for large angles of θ.

Ducting for whistler waves in a trough in VTF is analyzed in the same way as the ionospheric case. The line between ducted and non-ducted signals at $\theta = 0$ is the

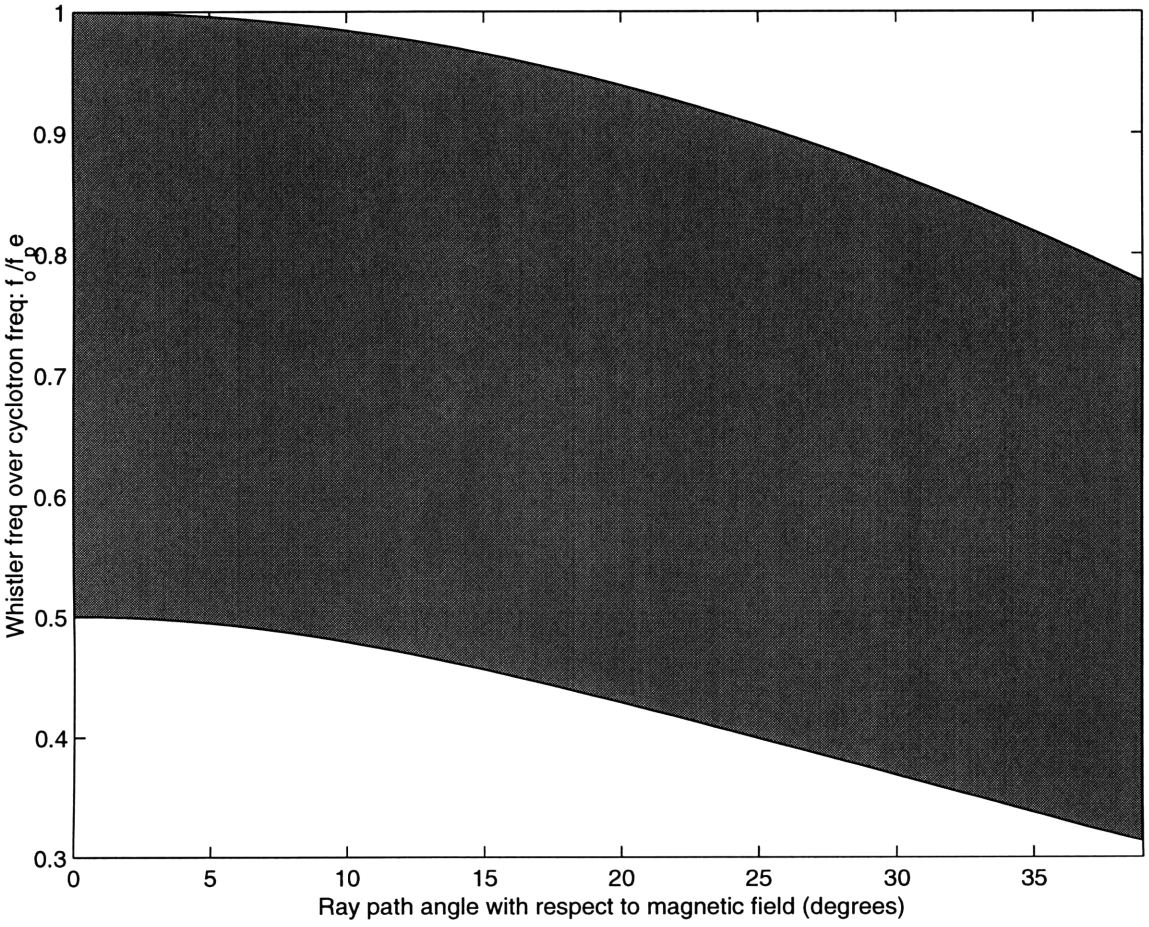

Figure 3-6: Ducting region for ionospheric whistler waves in a density depletion.

same as earlier in the chapter, but the ducting region is above the line, not below. This is shown in Figure 3-7.

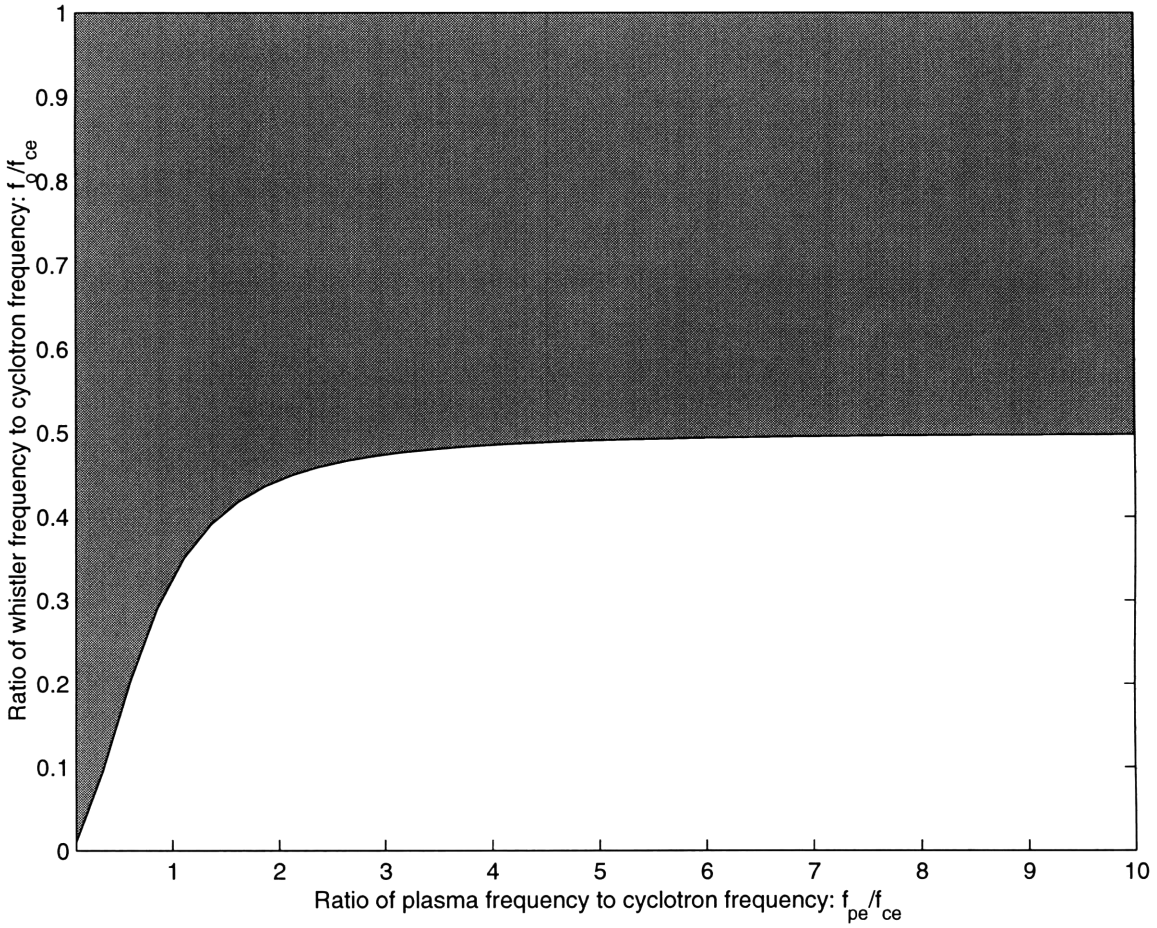

Figure 3-7: Ducting region for whistler waves in VTF in a density depletion.

In VTF the shape of the plasma is more conducive to crest ducting than trough ducting. A density trough ducts best when density increases in all directions in the plane perpendicular to wave propagation; conversely a density crest ducts best when density decreases in all directions in the plane. Plasmas in VTF do form this type of crest density configuration, however, they do not form troughs where density increases in every direction in the plane. In VTF density troughs, there are always several directions in which density continues to decrease.

3.3 Generation of Waves

In the ionosphere, whistler waves are generated by lightning. A flash of lightning produces a broad band of electromagnetic radiation. [10] The subsequent electromagnetic waves are either ducted along the magnetic field or their energy is dissipated in the plasma. Electrons in lightning are traveling fast enough to produce Čerenkov radiation. When the speed of an electron is greater than the phase speed of a wave, the electron will give off energy until its speed matches the phase speed of the wave. The energy radiated is Čerenkov radiation. Lightning-produced Čerenkov radiation is broadband in nature, and is higher in energy than bremmstrahlung. Bremmstrahlung or "braking radiation" is the energy released when a particle reduces velocity due to collisions. Čerenkov radiation's high energy is a result of the electrons losing energy efficiently without collisions. There is also the possibility that electrons will interact with each other and form ordered bunches of charge which release coherent Čerenkov radiation. Coherent Čerenkov radiation is even higher energy than its usual incoherent mechanism.

In VTF, the electron emitters are biased at about -360 volts. The equation for the phase speed of whistler waves comes from the dispersion relation for waves analyzed earlier in this chapter.

$$\frac{c^2k^2}{\omega^2} = \mu^2 = 1 - \frac{X}{1 - \frac{\sin^2\theta}{2\Lambda^2(1-X)} \pm \frac{1}{1-X}\left[\frac{\sin^4\theta}{4\Lambda^4} + \frac{\cos^2\theta}{\Lambda^2}(1-X)^2\right]^{\frac{1}{2}}} \tag{3.25}$$

Solving for the phase speed, $\frac{\omega}{k}$, yields:

$$\frac{\omega}{k} = \sqrt{\frac{c^2\left(1 - \frac{\sin^2\theta}{2\Lambda^2(1-X)} - \frac{1}{1-X}\left[\frac{\sin^4\theta}{4\Lambda^4} + \frac{\cos^2\theta}{\Lambda^2}(1-X)^2\right]^{\frac{1}{2}}\right)}{1 - \frac{\sin^2\theta}{2\Lambda^2(1-X)} - \frac{1}{1-X}\left[\frac{\sin^4\theta}{4\Lambda^4} + \frac{\cos^2\theta}{\Lambda^2}(1-X)^2\right]^{\frac{1}{2}} - X}} \tag{3.26}$$

Electrons at 360 eV travel at about 10^7 m/s. Assuming there is an energetic tail in the velocity distribution of electrons, a few particles will be around one keV in energy. Those energetic electrons travel at about 1.8×10^7 m/s. In order to produce Cerenkov radiation in the VTF vacuum chamber, the phase speed of whistlers must

be less than 1.8×10^7 m/s. In Figure 3-8, phase velocity is plotted with respect to θ

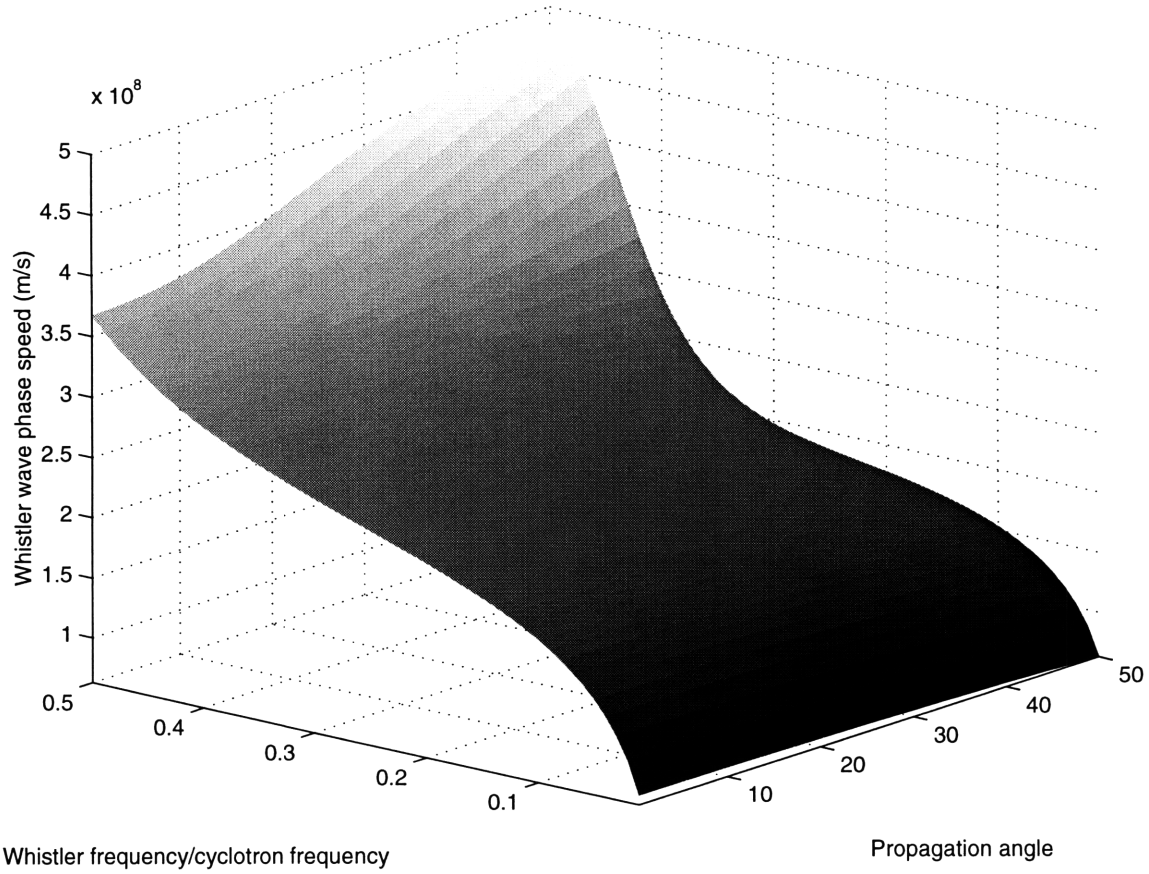

Figure 3-8: Whistler wave phase velocity vs. frequency and propagation angle

and Λ, in the range of parameter space where μ is real. The minimum phase velocity of whistler waves occurs at low frequencies and is about 6.3×10^7 m/s. Therefore, emitted electrons in VTF produce no Čerenkov radiation.

Since Čerenkov radiation is not produced in VTF, but gigahertz electromagnetic waves are detected, there must be some other mechanism that produces high frequency electromagnetic waves. This mechanism is bremmstrahlung or "braking radiation". As high speed electrons are generated by the emitter filaments, they collide with particles in the existing plasma, releasing energy. The energy from the high speed emitted electrons goes to many different mechanisms. There is the creation and heating of the plasma itself, for example. Neutral gas molecules have to be ionized to create a plasma. The free electrons are heated to maintain a temperature of several electron-volts. All the waves in an emitted beam plasma must originally get

their energy from the beams since that is the only plasma source. Low frequency electrostatic waves, such as ion-acoustic waves, are produced; and low frequency electromagnetic waves, such as lower hybrid waves, are also generated. Whistler waves and electrostatic waves around the plasma frequency are other types of waves that are produced and maintained by the electron beam's energy. The exact process for the energy transfer from the 360 eV emitted electrons to the various plasma waves has not been fully analyzed. However, qualitatively, the power radiated in the broadband whistler wave spectrum is related to the inverse of the total beam current. At high emitted beam currents, the electron temperature distribution is a drifting Maxwellian (Figure 3-9). This distribution preferentially gives its energy to electrostatic oscillations, especially low frequency ones, that require large electric fields to move large masses of charged particles. High beam currents produce higher density plasma and therefore require more energy to ionize the gas and heat the charged particles as well. Also higher beam currents yield higher plasma temperature. Bremmstrahlung energy is proportional to how much the electrons slow down and is a function of plasma temperature. Electrons basically give off energy until they are at the plasma temperature. With higher plasma temperature, electrons slow down less and release less energy into high frequency electromagnetic waves. With low emitted beam currents, the electron velocity distribution is Maxwellian but with a high energy tail, perhaps even a small second peak at a velocity several times higher than the average (Figure 3-9). This type of distribution tends to radiate broadband electromagnetic waves into gigahertz frequencies, in order to become more like a perfect Maxwellian. However, given the small number of energetic electrons and the high frequencies involved, whistler waves are the only plasma resonances that can absorb the radiation. Thus, beam currents of ten amps are expected to produce more energetic whistler waves than beam currents of 200 amps.

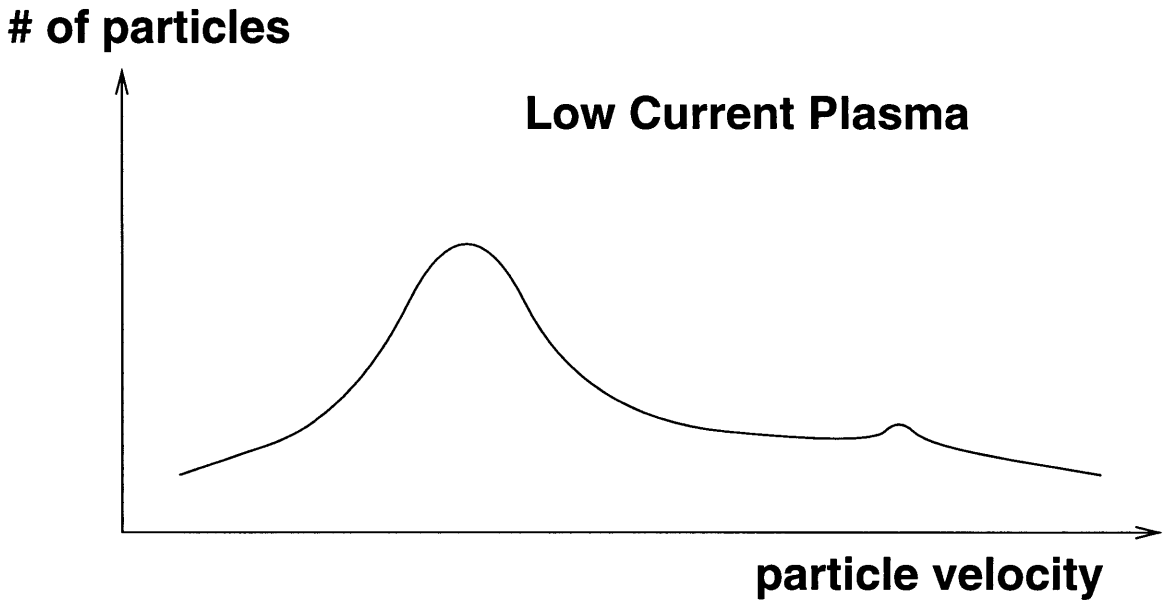

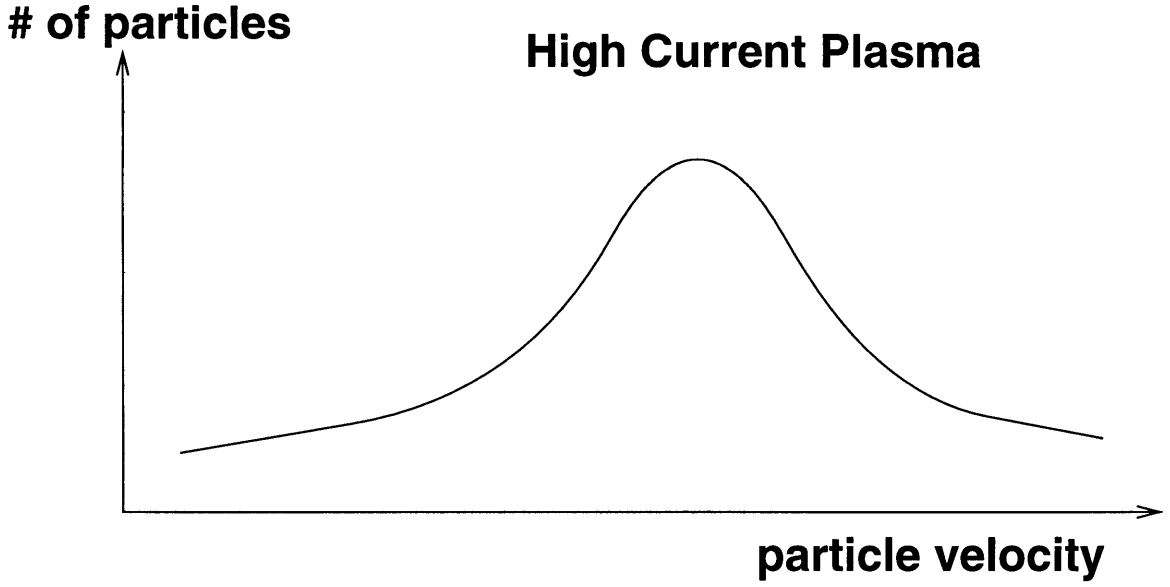

Figure 3-9: General velocity distributions for low and high beam current plasmas

3.4 Theoretical Conclusions

It is clear that electromagnetic wave ducting in a crest does not fully describe whistler wave propagation in VTF. Whistler wave ducting in a trough does not explain experimental results either. However, there are some limitations on ray theory that could cause a difference between theory and VTF experiments. The ray tracing analysis done in this chapter assumes that the number of wavelengths across a duct is much much greater than one. Also, it requires that density is approximately constant over a fraction of a wavelength. In the range of frequencies where a cutoff is observed in VTF (2-3 GHz), these conditions are not fully met. The size of a duct in VTF is about ten centimeters. At 2 GHz, the whistler wavelength in VTF is about sixteen centimeters, but the angle of propagation with respect to magnetic field is small, about ten degrees. So the effective wavelength across the duct is $\sin(\frac{\pi}{18}) \cdot 16 = 2.7$ cm. There are several wavelengths across the duct at that frequency, so the analytical results should be reasonable if not perfect. Under no conditions, in a plasma density crest, does the analysis predict ducting of electromagnetic waves above half the electron cyclotron frequency. Trough ducting does not completely explain experimental data either and in VTF plasmas, trough ducting is less ideal than crest ducting. A rough, qualitative analysis of wave generation for beam plasmas predicts that high frequency electromagnetic whistler waves are produced at both high and low beam currents. Emitted electrons are not energetic enough to produce Čerenkov radiation so the wave generation mechanism is bremmstrahlung. However, the radiation mechanism is different depending on the electron velocity distribution. Hence, low currents will produce more energetic whistler waves than high currents.

Chapter 4

Experimental Results

Many experiments were run in VTF to measure whistler waves. A variety of plasma conditions were observed and gigahertz electromagnetic waves were measured at a wide range of radii, plasma densities and magnetic field strengths. This chapter will attempt to present the important results of this data.

4.1 Plasma Density Contours

In order to get an idea of the exact ducting configuration of the plasma in VTF, a two-dimensional density scan was done. The radially scanning Langmuir probe was used to take single density profiles across the radius of the chamber. Then the vertical magnetic field was changed to move the plasma vertically. A whole set of density versus radius profiles, each with a different vertical field, was compiled to get a cross section of the plasma density. In Figure 4-1, this was done for a one-beam, 40-amp beam plasma. The shading goes from black, the least dense, to white, then most dense, representing plasma densities from 2×10^{16} ions/m^3 to 5×10^{17} ions/m^3.

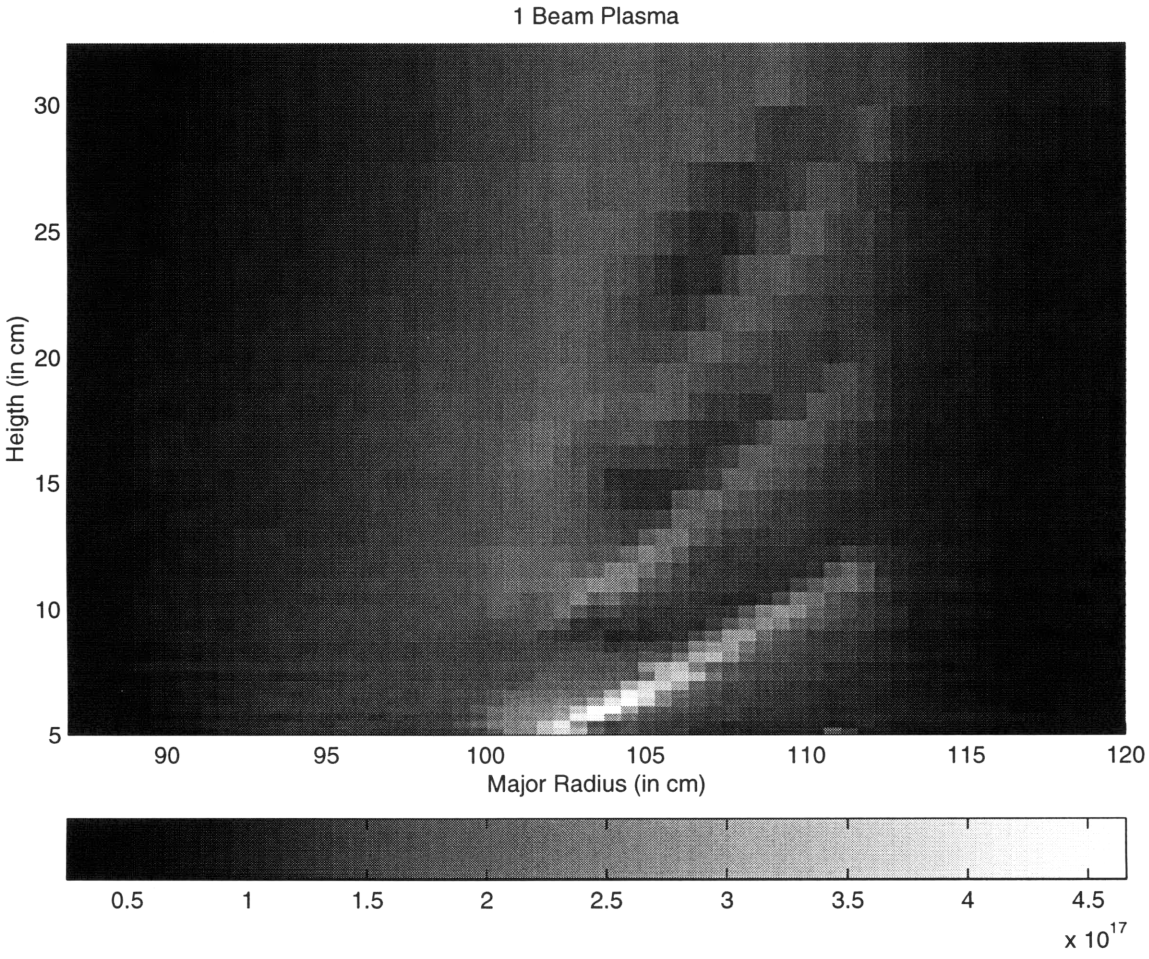

Figure 4-1: Two dimensional single-beam plasma density profile

It can be seen that the beams consist of long and thin "rungs", with a tilt that increases at higher rungs. This effect can be understood as follows. The beam emissions are about 15 cm long and 2 cm thick when they start out parallel to the bottom of the chamber. The emitted electrons travel along the background magnetic field which is the vector addition of the toroidal and vertical fields. The toroidal field strength is inversely proportional to radius, while the vertical field is constant, so the pitch angle of the magnetic field is higher at larger radii. Thus, as the beam travels along the background magnetic field and moves helically up the machine, each rung of the beam tilts more and more. This is seen in the two-dimensional contour. As the beam gets higher in the machine, its density decreases. This is also expected. As the electrons travel in successive circuits around the machine, away from the emitter, more of them escape the beam and run to the grounded walls of the chamber. As the beam gets higher in the chamber the beam current and therefore plasma density, becomes lower. It can also be seen that there are areas of decreased ionization in between beam rungs. These may be areas where trough ducting can occur. However, these areas are not ideal trough ducts. Radially outward and inward along the tilt of the beam, density does not quickly increase moving away from the duct. The beams are not ideal crests either, they are tilted rectangles, not horizontal cylinders. Still, there are several areas in the plasma where density decreases in all directions, and these can support crest ducting.

In addition to the single-beam, two-dimensional grayscale, a two-beam profile was also compiled. It was produced in the same manner as above, by running a set of density profiles with a different vertical field current each time. Both electron beam emitters were used at 40 amps of current each. The graph is shown in Figure 4-2. Again, the shading goes from black, least dense, to white, most dense, representing plasma densities from 1×10^{16} ions/m^3, to 6×10^{17} ions/m^3. Like the one-beam plasma, the density decreases as the electrons travel further up the machine and the beam current leaks to the side walls. However, there are no clear rungs in a two beam plasma. The plasma density is roughly homogeneous in the 100–110 cm radius range. This plasma configuration produces ducts that are close to an ideal crest. There

seems to be a slight decrease in ionization around 112 cm. Some trough ducting could occur there although density continues to decrease moving upward from the duct. From actual density measurements, the plasma density configuration in VTF, while not forming ideal ducts for electromagnetic waves, is sufficient for some ducting of waves in both crests and troughs.

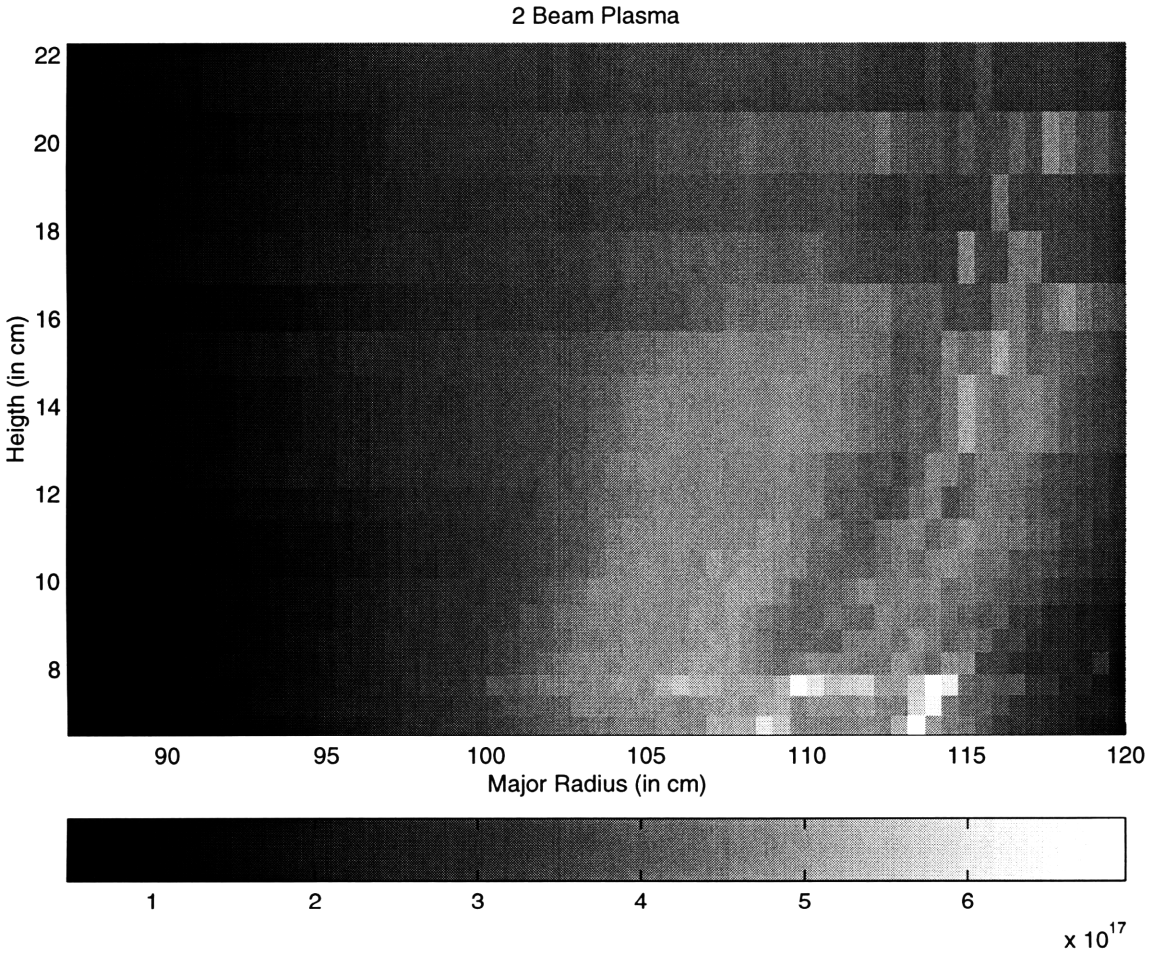

Figure 4-2: Two dimensional two-beam plasma density profile

4.2 Frequency Measurements with Microwave Plasma

When plasma was formed with only the 2.45 GHz microwave source, no whistler waves were detected. Around the pump wave, there obviously were some electromagnetic waves detected, but below that frequency, there were no whistler waves. This is shown

in Figure 4-3. The importance of this graph is that it shows that whistler waves are only generated by electron beams. In the 1–2.5 GHz range, in a microwave plasma, there are electrostatic oscillations around the local plasma frequency. If the loop probe did not shield out all electrostatic signals, it would detect waves below the pump wave in a microwave plasma. It does not, therefore it only detects electromagnetic waves, as we expect.

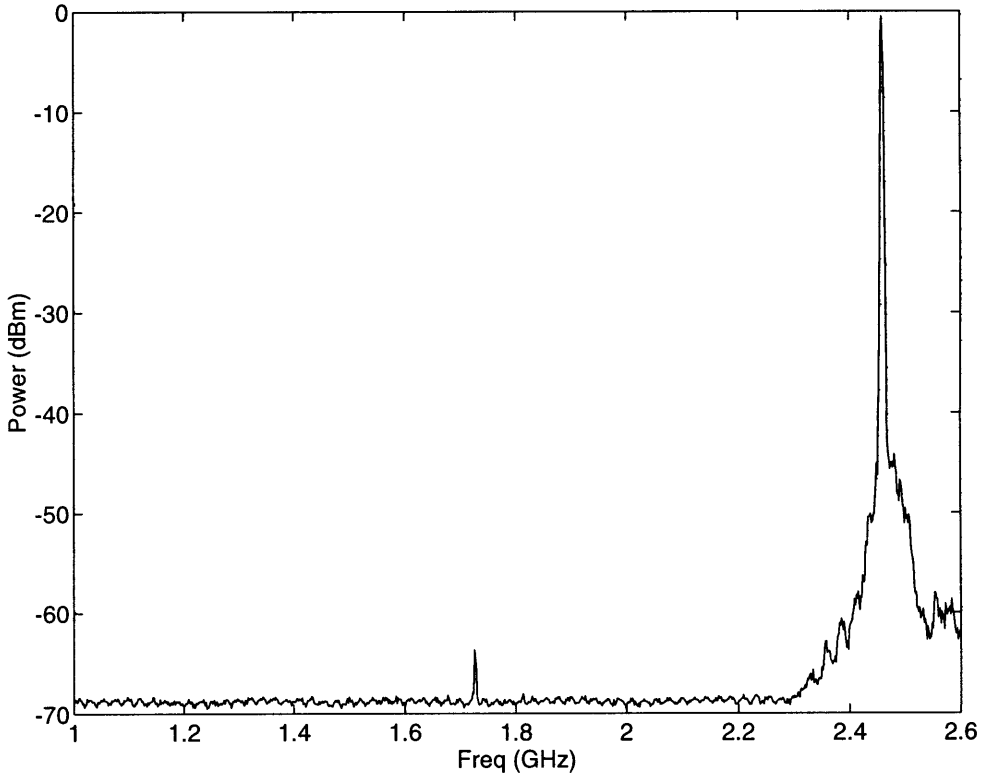

Figure 4-3: Power spectrum of microwave-only plasma

4.3 Variation in Whistler Wave Spectra with Density

Variations in whistler cutoff frequency with changing density were examined using low current, single-beam shots. In one shot, density and whistler spectra were measured

with no microwave. In the next shot, all conditions were identical except the 2.45 GHz microwave was turned on. The beam currents, field strengths, probe locations and measurement devices were kept constant for all shots. The beam current was sufficiently low such that the density it produced was an order of magnitude lower than the microwave plasma density. So without the microwave, there was a low density plasma with crests for ducting and a source of electromagnetic waves. With the microwave, there was a higher density plasma with a crest for ducting and a source of electromagnetic waves. The main differences between the two shots were the background plasma density and the shape of the density profile. The "beam only" shot had a background density of 7×10^{15} ions/m^3, while the "microwave plus beam" shot had a background density of 1.5×10^{16} ions/m^3. As mentioned in Chapter 1, the beam plasmas have a sharper density peak than microwave plasmas (see Figure 2-3 and Figure 2-4). It can be seen in Figure 4-4 that for both density configurations, cutoff frequency is about the same. With the 2.45 GHz microwave on, there is a peak in the spectrum at 2.45 GHz, but it does not seem to affect the shape or cutoff frequency of the whistler wave spectrum. This seems to indicate that for these two shots, with significantly different plasma density structures, a similar mechanism is ducting the whistler waves.

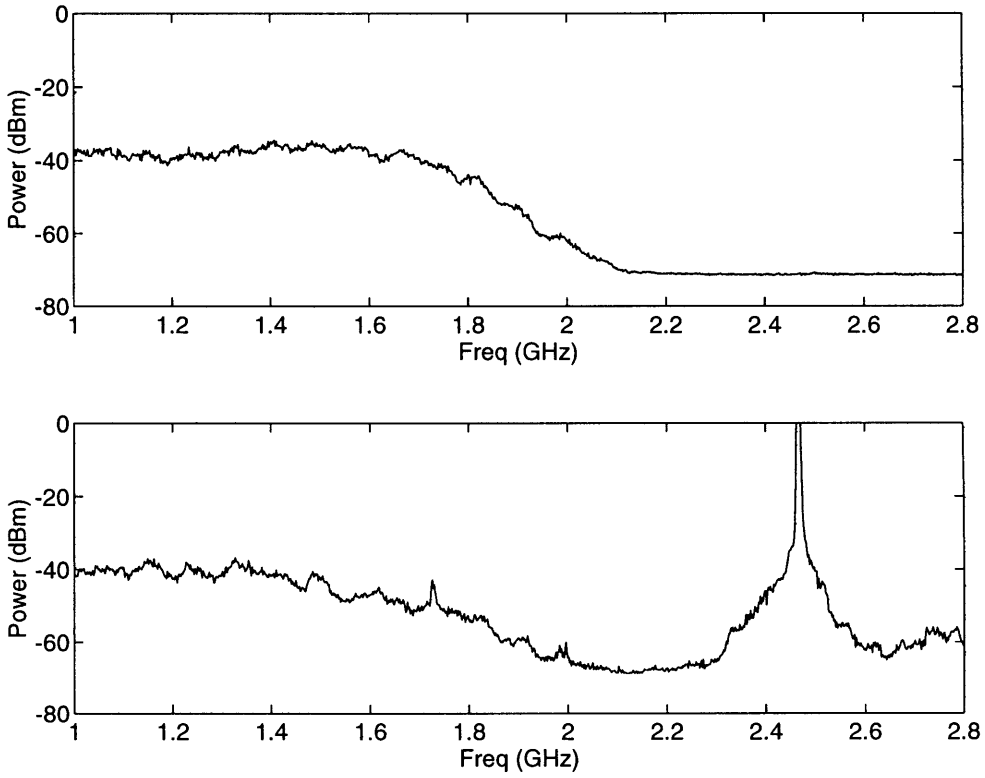

Figure 4-4: Power Spectra. Top: no microwave, plasma density $7 \times 10^{15}/\mathrm{m}^3$, Bottom: with microwave, plasma density $1.5 \times 10^{16}/\mathrm{m}^3$

4.4 Whistler Wave Cutoff Frequency versus Cyclotron Frequency

In VTF the magnetic field, and therefore the electron cyclotron frequency, ω_{ce}, changes with major radius. The toroidal field is inversely proportional to major radius. For constant Λ, cutoff frequency should decrease with increasing major radius, as ω_{ce} decreases. This is shown in Figures 4-5 and 4-6.

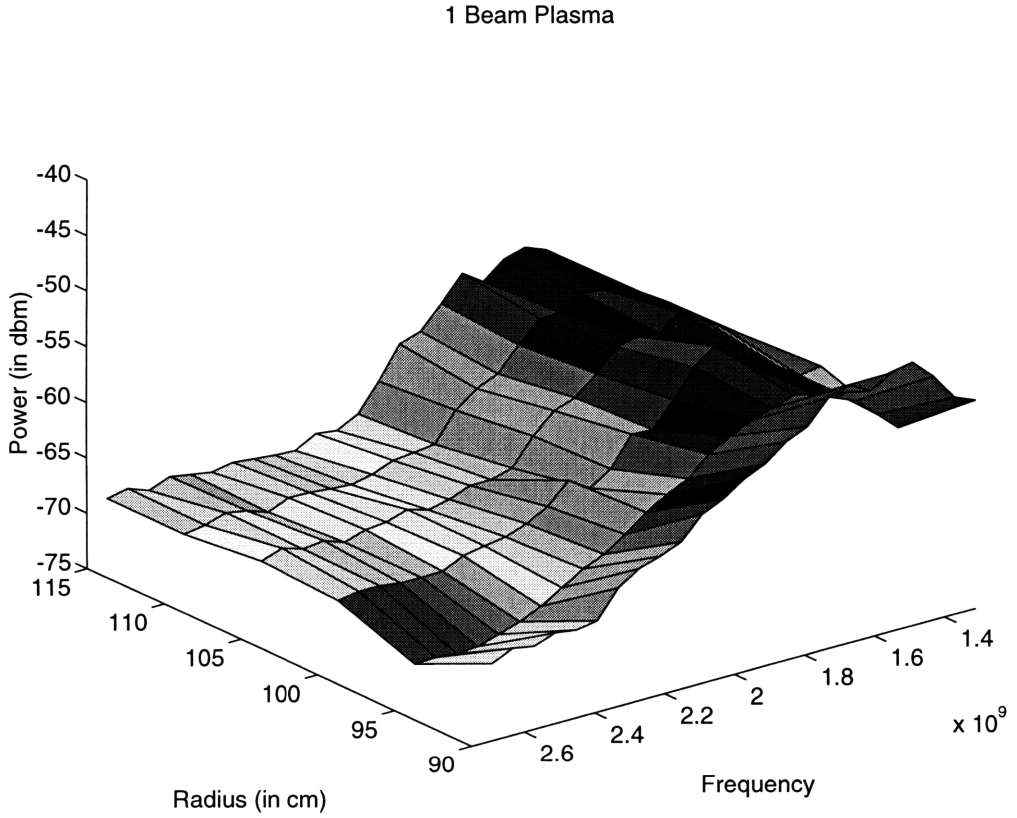

Figure 4-5: Power vs. frequency vs. major radius for whistler waves in a one-beam plasma

It can be seen in Figure 4-5 that cutoff frequency increases with increasing magnetic field, (decreasing major radius). This is what was expected. The magnetic field at a radius of 100 cm is about 0.08 tesla so ω_{ce} is 2.24 GHz. Cutoff frequency at that radius is measured to be 1.95 GHz, which is $.87\omega_{ce}$.

In Figure 4-6 the cutoff frequency also increases with increasing magnetic field, (decreasing major radius), as expected. The magnetic field at a radius of 100 cm is about 0.08 tesla so ω_{ce} is 2.25 GHz. Cutoff frequency at that radius is measured to be 2.24 GHz which is approximately ω_{ce}. It is clear from these graphs that above a certain frequency, no waves are detected. It is also obvious that the cutoff frequency changes with radius. Furthermore, these graphs show that a one-beam plasma and a two-beam plasma do not have identical whistler wave spectra.

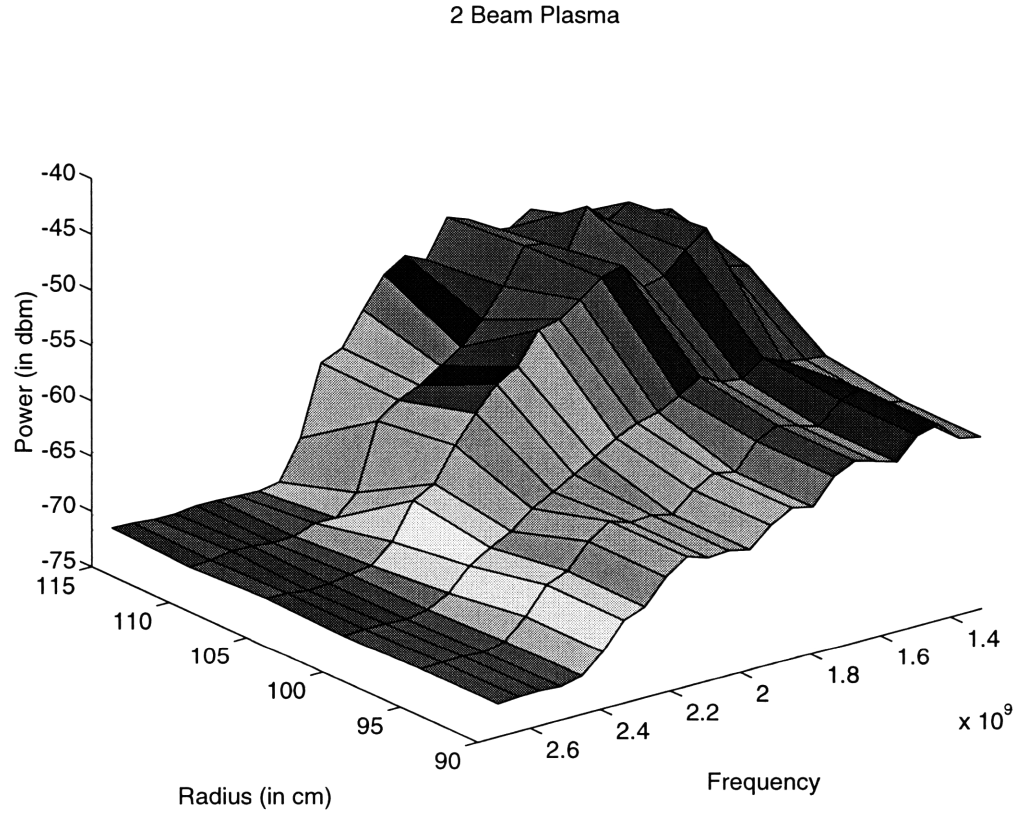

Figure 4-6: Power vs. frequency vs. major radius for whistler waves in a two-beam plasma

Other experiments at fixed radius and changing magnetic field have shown that cutoff frequency is indeed proportional to magnetic field, as in Figure 4-7.

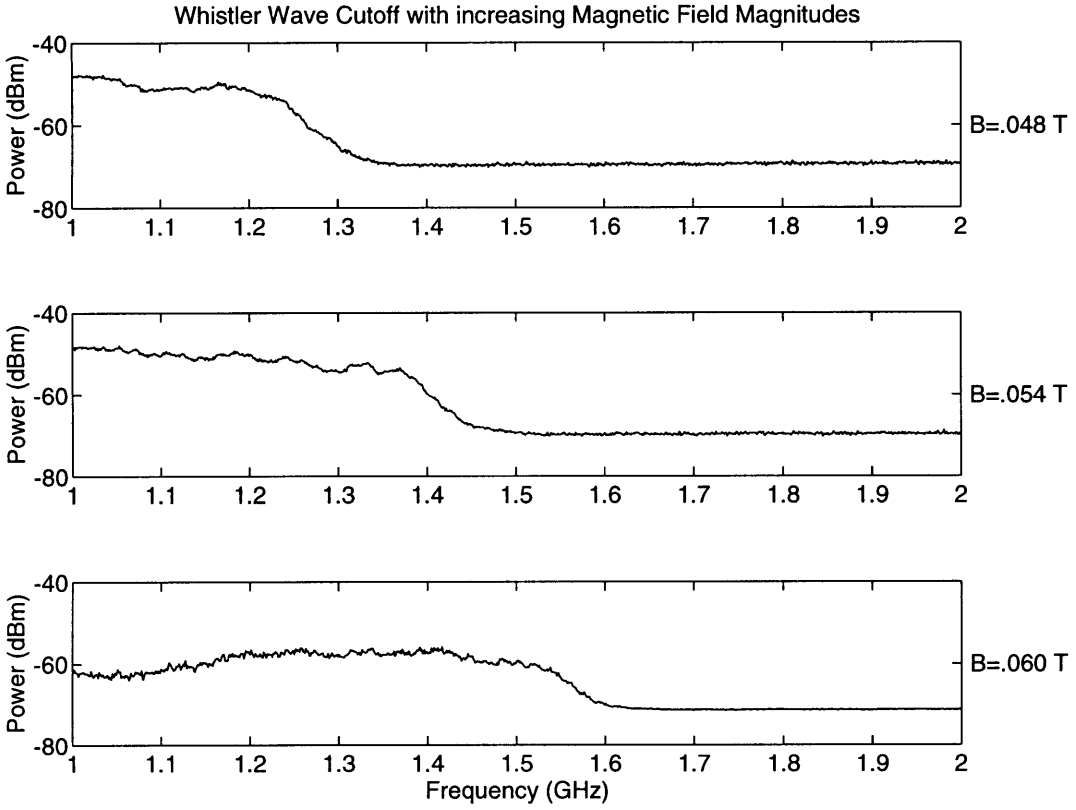

Figure 4-7: Changing cutoff frequency with changing magnetic field

Figure 4-8 is an example of a spectrum taken during a single shot. Magnetic field was 0.1 Tesla at the probe tip when this spectrum was taken. Therefore ω_{ce} was 2.78 GHz and waves were detected up to the cyclotron frequency. Notice that the power is not constant over the frequencies where waves are seen. There seems to be a bump between 1.5 GHz and the whistler cutoff. Perhaps the ducting mechanism is more efficient in that range.

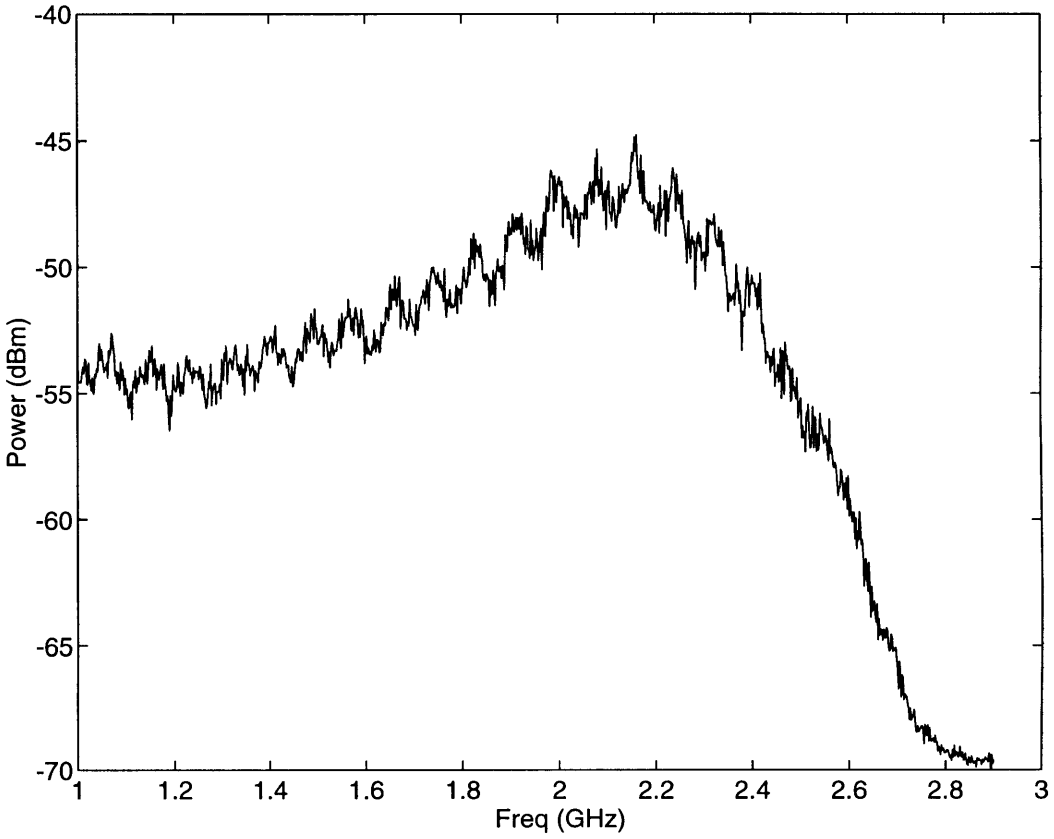

Figure 4-8: High frequency spectrum of whistler waves

4.5 Whistler Wave Power Dependence on Beam Current

As mentioned in a previous chapter, it was theorized that the detected power of whistler waves should be different for different emitter currents in the electron beam-produced plasmas. [11] This was confirmed in VTF experiments. The following graph, Figure 4-9, shows spectra taken by the loop probe, at the same radius and toroidal field, but with different electron beam currents. These spectra were taken with a single

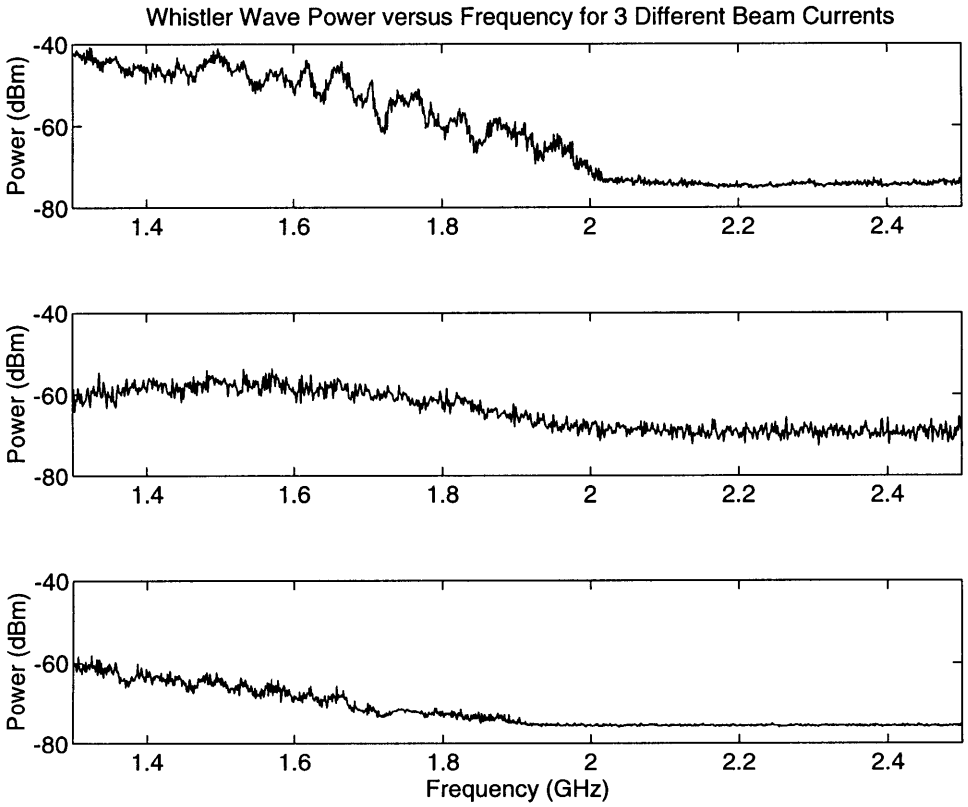

Figure 4-9: Whistler wave spectra at various beam currents.

electron beam filament firing. Going from the top plot to the bottom, the emitted currents were 10 amps, 40 amps and 200 amps. It is clear that the lowest emitted current generated the most energetic whistlers and the highest current generated the least energetic. As mentioned in the previous chapter, this was expected because as current increases, plasma density increases and as plasma density increases more

energy goes to electrostatic plasma modes and heating and generating the plasma. In other words, with higher density and temperature, much more energy is needed to maintain the plasma and much less energy goes into bremmstrahlung.

4.6 Experimental Results Summary

Experiments in VTF show several things. First, there are gigahertz electromagnetic waves produced during a beam plasma shot. These waves have an upper cutoff frequency, i.e. there is a frequency above which they are not seen. This cutoff frequency is proportional to magnetic field, but independent of the magnitude of plasma density. One beam and two beam plasmas do not have the same density configuration and do not generate the same whistler wave spectra. Higher beam currents produce higher plasma density and temperature, but lower power whistler waves, and vice versa for lower beam currents. Plasmas generated only by microwave ECRH do not produce whistler waves. Experimental results generally agreed with theoretical predictions.

Chapter 5

Conclusions and Future Experiments

5.1 Further Experiments

As with most research, there is always more work that could be done. A scanning probe that could measure electromagnetic waves across the radius of the machine in a single shot would yield useful data. Three orthogonal loops could be used to measure the exact direction of propagation of waves in the chamber. Rebuilding the electron beam power supplies to generate higher beam currents, and regulating currents more precisely would allow more understanding of wave generation. Inserting a probe near the beam filament and comparing that information to a probe further away could shed more light on the propagation of whistler waves. It is hoped that researchers at VTF will soon be better able to understand laboratory whistler wave phenomena.

5.2 Conclusions

It is clear that beam plasmas in VTF generate electromagnetic waves in the gigahertz range. It is also obvious that there is an upper cutoff frequency to these waves, above which none are detected. Experiments show conclusively that the upper whistler wave cutoff is inversely proportional to the background magnetic field and therefore,

the cyclotron frequency. Cutoff frequency is not related to the amount of background plasma density, but does depend on the shape of the plasma density profile. One-beam and two-beam plasmas have different density configurations and generate slightly different whistler wave spectra.

Theoretical analysis was done on electromagnetic waves propagating nearly parallel to the background magnetic field in laboratory plasmas. The results of the analysis showed that in a crest of increased plasma density, waves are not ducted above half the cyclotron frequency. The results also showed that in a trough of decreased plasma density waves could be ducted from half the cyclotron frequency up to the cyclotron frequency.

Since experimental results reveal a distinct upper cutoff frequency around the cyclotron frequency while showing waves well below half the cyclotron frequency, there must be some combination of crest and trough ducting going on in the plasma chamber. High frequency electromagnetic waves travel in small ducts in the complex density configuration in the chamber. When the waves move out of the ducts they propagate until they are reflected by one of the chamber walls. The waves can be detected at large radii where there is little plasma as long as they are below the cyclotron frequency at that point. Anytime that the waves are above the cyclotron frequency, the index of refraction becomes purely imaginary and the waves dissipate. [9] However, if the waves are not dissipated, they can re-enter a duct after they reflect off a chamber wall. Since the size of plasma ducts is comparable to the wavelength of the waves that propagate through them, whistler waves can easily escape the duct and be detected outside the duct.

Whistler waves are defined as electromagnetic waves in the range of frequencies up to the cyclotron frequency, which propagate along the background magnetic field in a plasma. The name comes from the fact that higher frequencies propagate faster in the plasma. The result is that for a fixed observer and a point source of broadband radiation, the observer hears a pitch of descending frequency; a whistle. In the atmosphere, these waves are only ducted up to half the cyclotron frequency. In VTF laboratory experiments, they are detected up to the cyclotron frequency. Electron

beam filaments in the plasma chamber generate these high frequency electromagnetic whistler waves. Due to the mechanism of generating and heating the plasma, and transferring energy to various resonant plasma waves, lower beam currents yield higher power whistler waves. The waves propagate and are ducted in both small crests and small troughs in the chamber. As a result of the small size of the ducts, waves can leave a duct, reflect off the chamber wall and re-enter another duct. Thus, waves can be detected across the entire radius of the machine all the way up to the cyclotron frequency.

Bibliography

[1] Helliwell, R.A., *Whistlers and Related Ionospheric Phenomena*, Stanford University Press, Stanford, CA, 1965.

[2] Carpenter, D.L., Ducted Whistler-Mode Propagation in the Manetosphere; A Half-Gyrofrequency Upper Intenstiy Cutoff and Some Associated Wave Growth Phenomena, *Journal of Geophysical Research*, Vol. 73, No. 9, Pages 2919-2928, May 1, 1968.

[3] Smith, R.L., Propagation Characteristics of Whistlers Trapped in Field-Aligned Columns of Enhanced Ionization, *Journal of Geophysical Research*, Vol. 66, Page 3699, 1961.

[4] Beals, D.F., *Characterization of Hot Cathode Helimak Plasmas*, MIT Electrical Engineering Department Master's Thesis, 1994.

[5] Hutchinson, I.H., *Principles of Plasma Diagnostics*, Cambridge University Press, Cambridge, 1987.

[6] Moriarty, D.T., *Laboratory Studies of Ionospheric Plasma Processes with the Versatile Toroidal Facility (VTF)*, MIT Nuclear Engineering Department Sc.D. Thesis, 1996.

[7] Chen, F. *Introduction to Plasma Physics and Controlled Fusion*, Plenum Press, 309-315, 1984.

[8] Riddolls, R.J., *Whistler Ducting*, Report to the MIT Ionospheric Research Group, July 8, 1997.

[9] Farrell, W.M., D.A. Gurnett, P.M. Banks, R.I. Bush, and W.J. Raitt, An Analysis of Whistler Mode Radiation From the Spacelab 2 Electron Beam, *Journal of Geophysical Research*, vol. 93, No. A1, Pages 153-161, January 1, 1988.

[10] Kelley, M.C., J.G. Ding, and R.H. Holzworth, Intense Ionospheric Electric and Magnetic Field Pulses Generated by Lightning, *Geophysical Research Letters*, Vol. 17, No. 12, Pages 2221-2224, November 1990.

[11] Porkolab, M., V. Arunasalam, N.C. Luhmann Jr., Plasma Heating in the Presence of Parametric Instabilities in a Magnetic Field, *Plasma Physics*, Vol, 17, Pages 405-419, 1975.